THE UNIMOLECULAR DISSOCIATION OF Rg_2I_2

$Rg = (He, Ar, Kr, Xe)$

By

JEFFREY CRAIG FUSON

Bachelor of Science

University of Oklahoma

Norman, Oklahoma

1981

Submitted to the Faculty of the
Graduate College of the
Oklahoma State University
in partial fulfillment of
the requirements for
the Degree of
MASTER OF SCIENCE
December, 1991

Thesis
1911
Paris

THE UNIMOLECULAR DISSOCIATION OF Rg_2I_2

Rg = (He,Ar,Kr,Xe)

Thesis Approved:

Lionel M. Raff
Thesis Advisor

Paul W. Harmon

Donald L. Thompson

Thomas C. Collins
Dean of the Graduate College

ACKNOWLEDGEMENTS

I would like to express my deepest thanks to the following people who served as members of my advisory committee: Drs. L.M. Raff, D.L. Thompson, and P.A. Westhaus. I thank you all for guidance, help, and encouragement throughout my graduate career. Thanks also go to the entire Physical Chemistry faculty for the same.

I would also like to thank my colleagues Tommy Sewell, Eric Wallis, and Yue Qin for their help and support. Finally, special thanks go to Drs. K.D. Berlin and E.J. Eisenbraun for their help and support.

TABLE OF CONTENTS

Chapter		Page
I.	LITERATURE REVIEW	1
	Van der Waals Photochemistry	1
	Brief Overview of Beam Experiments	2
	Previous Theroretical Treatment of RgX_2 (X=halogen)	3
	Rationale for the Present Study	6
II.	METHODS	7
III.	RESULTS AND DISCUSSION	13
BIBLIOGRAPHY		48

LIST OF TABLES

Table		Page
1.	Potential Energy Parameters	9
2.	Rare Gas = Agron	15
3.	Rare Gas = Krypton	16
4.	Rare Gas = Xenon	17
5.	Rare Gas = Helium	18

LIST OF FIGURES

Figure		Page
1.	Schematic of internuclear distances for Rg_2I_2	7
2.	Transition from the X^1S to the B^3P electronic state	10
3.	Plot of $\ln(N/N_0)$ vs. dissociation time for Ar at 0.609 eV	20
4.	Plot of $\ln(N/N_0)$ vs. dissociation time for Ar at 0.620 eV	21
5.	Plot of $\ln(N/N_0)$ vs. dissociation time for Ar at 0.640 eV	22
6.	Plot of $\ln(N/N_0)$ vs. dissociation time for Ar at 0.660 eV	23
7.	Plot of $\ln(N/N_0)$ vs. dissociation time for Kr at 0.609 eV	24
8.	Plot of $\ln(N/N_0)$ vs. dissociation time for Kr at 0.620 eV	25
9.	Plot of $\ln(N/N_0)$ vs. dissociation time for Kr at 0.640 eV	26
10.	Plot of $\ln(N/N_0)$ vs. dissociation time for Kr at 0.660 eV	27
11.	Plot of $\ln(N/N_0)$ vs. dissociation time for Xe at 0.609 eV	28
12.	Plot of $\ln(N/N_0)$ vs. dissociation time for Xe at 0.620 eV	29
13.	Plot of $\ln(N/N_0)$ vs. dissociation time for Xe at 0.640 eV	30
14.	Plot of $\ln(N/N_0)$ vs. dissociation time for Xe at 0.660 eV	31
15.	Plot of $\ln(N/N_0)$ vs. dissociation time for He at 0.609 eV	32
16.	Least-squares fit for Plot No. 15	33
17.	Plot of number of occurrences vs. recoil energy for Ar at 0.609 eV	35
18.	Plot of number of occurrences vs. recoil energy for Ar at 0.620 eV	36
19.	Plot of number of occurrences vs. recoil energy for Ar at 0.640 eV	37
20.	Plot of number of occurrences vs. recoil energy for Ar at 0.660 eV	38
21.	Plot of number of occurrences vs. recoil energy for Kr at 0.609 eV	39

Figure Page

22. Plot of number of occurrences vs. recoil energy for Kr at 0.620 eV..... 40

23. Plot of number of occurrences vs. recoil energy for Kr at 0.640 eV..... 41

24. Plot of number of occurrences vs. recoil energy for Kr at 0.660eV 42

25. Plot of number of occurrences vs. recoil energy for Xe at 0.609 eV 43

26. Plot of number of occurrences vs. recoil energy for Xe at 0.620 eV 44

27. Plot of number of occurrences vs. recoil energy for Xe at 0.640 eV 45

28. Plot of number of occurrences vs. recoil energy for Xe at 0.660 eV 46

29. Plot of internal energy vs. excitation energy for Ar, Kr, and Xe..... 47

CHAPTER I

LITERATURE REVIEW

Van der Waals Photochemistry

Many chemical systems may be combined under common laboratory conditions without a "chemical" bond being formed(1). However, van der Waals (vdW) interactions always occur, and thus, the number of vdW systems found in nature is very large. In spite of this, the range of conditions under which vdW interactions occur is more circumscribed than that of systems with chemical bonds, owing to the shallowness of the vdW potential-energy well.

An exemplary vdW complex is comprised of an "ordinary" chemically bound molecule (the "substrate") weakly bonded to one or more rare gas (Rg) atoms by vdW forces. Vibrations within the complex may be classified into "chemical" modes and "vdW" modes. The rationale for this lies in the fact that vdW bonds are much weaker than chemical bonds, and chemical modes with nominal excitation (as little as one quantum above the zero-point) are more energetic than the total vdW binding energy. Energy from the chemical vibrational modes (i.e., the vibrations in the chemically bonded substrate) may be redistributed to the vdW vibrational modes. Vibrational energy redistribution will eventually lead to the complex's dissociation. This process has been called vibrational predissociation (VPD) (2). Two aspects of VPD have been investigated for a number of systems: intramolecular energy transfer from the initial storage mode, and energy distribution in the available degrees of freedom of the fragments produced in dissociation.

Vibrational predissociation offers unusually attractive features for both theoretical and experimental study (2). The vibrational excitation energy needed in VPD is minimal, and preselected, individual, vibrational and rotational levels may be subjected to optical selection studies. Along with a well-defined and controllable excitation process, vdW molecules offer a reasonably simple adiabatic potential energy surface which may be constructed from spectroscopic data (3). Thus, the investigation of a vdW bond is more amenable to a theoretical treatment than that of an "ordinary" chemical bond. Moreover, there are features of vdW photochemistry that overlap ordinary photochemistry (4). Complexes are present in small concentrations in bulk gas samples, so that their spectra can in principle be measured under equilibrium conditions with conventional techniques.

Brief Overview of Beam Experiments

Supersonic jet spectroscopy is useful in the study of vdW molecules. Supersonic expansion provides a means for the preparation of a low-temperature environment where the most-probable relative kinetic energy is much less than that of characteristic vdW binding energies, which are usually smaller than kT if T is on the order of 300 K. Under these conditions, the nascent vdW complexes are stable with respect to collisions with the surrounding gas. Supersonic expansion also simplifies the spectrum by depopulation of rotational and vibrational states.

In a pioneering study, Smalley et al. (5) prepared HeI_2 vdW complexes and obtained laser-induced fluorescence excitation spectra of the B <-- X transition . They determined that VPD is the predominant decay mechanism of the vibrationally excited B states of HeI_2. They also found that the vdW complex was remarkably long-lived, with a lifetime of on the order of 2.0×10^{-10} sec, or about 1000 vibrational periods of the I_2 stretching vibration, in spite of the presence of vibrational energy that is about 0.11 eV in excess of the dissociation limit. Their results demonstrated the weakness of the coupling

between the I_2 and the Rg-I_2 stretching modes. The vibronic structure of this complex was found to be closely akin to that of free I_2, but with the bands blue shifted slightly (by about 3.7 cm^{-1}). Since the vdW bond has little effect on the I_2 vibrational motion, the molecule could be treated in terms of two simple local modes of vibration: the I-I vibration and the Rg-I_2 vibration.

The work of Levy et al. further exploited the possibilities of vdW molecules in the study of the microscopic details of bond breaking and formation (6,7). In the past few years, the technique of spectroscopy in supersonic molecular beams or free jets has been used in a wide variety of applications. The spectral simplification that results when the internal degrees of molecular freedom are cooled improves the resolution and allows the analysis of spectra that would be hopelessly complicated had they been studied in a static gas. The cold environment of a supersonic expansion allows the preparation and study of a weakly bound or reactive species, such as van der Waals molecules, that are difficult or impossible to study any other way. Observation of vibrational predissociation was first reported in I_2He (5). The lifetime for the process was deduced from the line width of the fluorescence excitation spectrum, and the lifetime was measured as a function of the vibrational state of the I_2 stretch that was originally excited.

The results are in the range of tens to hundreds of picoseconds, the lifetime becoming shorter for higher excitation. This lifetime corresponds to hundreds of vibrational periods of the iodine stretch.

Previous Theoretical Treatment of RgX_2 (X=halogen)

Beswick and Jortner (8) conducted a collinear quantum mechanical study for a hypothetical triatomic molecule, X-BC. Using harmonic and Morse potentials to generate zeroth-order wave functions, they obtained closed analytical expressions for the rate of vibrational predissociation and for the vibrational distribution of products. They

established an energy-gap law which predicted that the VPD rate would be enhanced by a close matching of the BC vibrational frequency, (which breaks the molecular complex), with the effective stretching frequency of the vdW bond. Further, they extended this theory to account for VDP of T-shaped vdW complexes. The T-shaped complexes were not amenable to analytical solution, however, and numerical integration of the close-coupling equations was necessary to obtain VPD rates.

Delgado-Barrio and co-workers (9) studied the RgI_2 system using both classical trajectory and quasiclassical sudden approximation methods. They obtained VPD rates as a function of the vibrational quantum number. Halberstadt et al. (10) used close-coupling methods to study vibrational predissociaton of the $NeCl_2$ system quantum mechanically. At large distances, the potential interactions were switched to an anisotropic van der Waals interaction with R^{-6} and R^{-8} dependence. This approach yielded calculated lifetimes and rotational distributions of the Cl_2 fragments in qualitative agreement with experimental values (10).

In a quasiclassical trajectory (QCT) study of collinear HeI_2, Woodruff and Thompson (11) demonstrated that QCT vibrational predissociation rate coefficients were in good agreement with the quantum mechanical VPD rate coefficients obtained by Beswick and Jortner (2), as well as the experimental results of Levy et al., (4,5). This study conclusively established the utility of the classical mechanical approximation for the VPD process.

Theoretical studies of the cage effect were initiated by Rabinowitch and Wood (12). The concept itself was introduced by Frank and Rabinowitch (12) to explain the decrease in photochemical production of free radicals in solution. For example, a diatomic molecule promoted to an excited state above the dissociation limit will, barring photon emission or collisions with other molecules, dissociate to yield free atoms. Yet in a liquid or dense gas, the dissociating atoms may be "caged" in by adjacent molecules and be compelled to

recombine before permanent dissociation can occur. Recombination is facilitated by the transfer of kinetic energy from the dissociating atoms to the adjacent "cage" atoms.

Murrell et al. (13) used QCT methods to study molecular iodine excited to the repulsive limb of the $A(^3\Pi_1)$ state caged by 22 rare gas atoms. They found that the Rg atoms could effectively stabilize the iodine sufficiently for stabilization to occur. Saenger and co-workers (14) observed a "one-atom" cage-effect with dissociation of M-I_2 (M = Ar, N_2, etc.) to yield bound I_2 molecules in the electronically excited B state. The cage effect is well-known in solutions, matrices, and high-pressure gases, however, its observation in a vdW complex under collision-free conditions (effectively a "one-atom cage") was seen for the first time. Valentini and Cross (15) reported similar results shortly afterwards. They excited a Van der Waals molecule above the dissociation limit, which then allowed the excess energy to be distributed between the internal degrees of freedom and the kinetic energy of the recoiling fragments. They observed molecular iodine in vibrational levels ($23 \leq v' \leq 49$) from 800 cm^{-1} to more than 2300 cm^{-1} below the energy of the initially excited iodine. Since energy transfer of this magnitude is not observed upon excitation of the ArI_2 system to bound I_2 B state levels, they attributed the result to the cage effect. Saenger et al. (14) were unable to obtain any information about the vibrational distribution of the I products due to poor resolution of the fluorescence spectrum.

In a QCT study, NoorBatcha et al. (16) obtained detailed product vibrational distributions for the unimolecular dissociation of RgI_2 (Rg = Ar,Kr,Xe). In accordance with the experimental data, they found that a significant fraction of RgI_2 "unbound" complexes dissociated only to recombine forming molecular iodine. Significantly, they also determined that the efficiency of energy transfer increased with increasing Rg atomic mass. This is in reasonable accord with a simple hard-sphere impulsive model for energy transfer, in which energy transfer is maximized for atoms with equal mass. A large fraction of I_2 molecules were formed with energy well below the dissociation limit, indicating that an effective vibrational energy transfer process was occurring. As the initial

excitation energy increased, the fragment energy distributions shifted toward the higher energy region.

Schatz et al. (17) extended the study of the RgI_2 system to include a second Rg atom. The complexes studied were Rg-Rg'-I_2 (Rg,Rg' = He,Ne) and He-Ne-I-I, a collinear system. Their results showed significant dynamical correlation effects of the rare gas atoms on each other despite the negligible direct interaction between them. Time-dependent self-consistent field studies and QCT studies were in agreement for rate constants, branching rates, and the variation produced by change in the rare gas. They did not, however, obtain detailed product vibrational distributions.

Rationale for the Present Study

Phillippoz, van den Bergh, and Monot (18) studied the photodissociation of RgI_2 (Rg = He,Ne,Ar,Kr, and Xe) for several excitation wavelengths above the B-state dissociation limit. They found that Ar yielded the lowest fragment recoil energy of the series. This would imply greater energy transfer efficiency for He, in disagreement with the classical trajectory results of NoorBatcha et. al. (16) and the expanded data reported by Valentini and Cross (15). While reasonable care was exerted to ensure the bonding of a single Rg atom with the I_2 molecule, it seems unlikely that He, an order of magnitude less massive than Ar and with significantly lower van der Waals interactions, would show a greater energy transfer efficiency. In our view, it was more probable that the enhanced transfer capability of He is due to the accidental production of higher homologues, such as Rg_2I_2, or Rg_3I_2. This anomalous result (18) has provided the impetus for the present study. We intend to examine the VPD dynamics for Rg_2I_2 (Rg= He,Ar,Kr,Xe) to determine reaction mechanisms, VPD rate coefficients, and magnitude of the cage effect. These calculations are therefore a generalization of this previously reported by Schatz, et. al. (17) in that the full three-dimensional dynamics of Rg_2I_2 will be investigated.

CHAPTER II

METHODS

QCT methods have been described elsewhere (19). We shall therefore describe only those aspects which are unique to this problem. The Hamiltonian is given by

$$(1) \qquad H = \sum_{i=1}^{4} (1/2M_i) P_i^2 + \sum_{j=1}^{6} V_j (R_j),$$

where P_i is the i^{th} atomic momentum in cartesian coordinates, M_i is the i^{th} atomic mass, V_j is the j^{th} intermolecular potential, and R_j is the j^{th} internuclear distance. The R_j are defined in Figure 1.

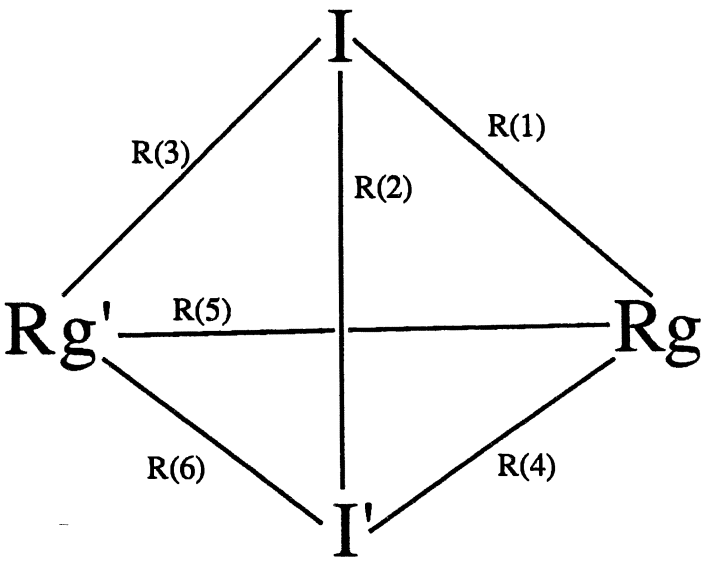

Figure 1. Schematic of Internuclear Distances for Rg_2I_2

The V_j are simple pairwise Morse functions

$$V_j(R_j) = D_j\{1 - \exp(-\alpha_j (R_j - R_j^o))\}^2 . \quad (2)$$

Studies of systems such as Rg_2I_2 using a Hamiltonian of the form of Eq. (1) are now feasible because pair forces are known to a very high degree of accuracy. Howard, Roberts, and DelleDonne (20) , in a study of $Ar + Ar_2^*$, demonstrated the adequacy of pairwise potentials for treating VDW systems. Consequently we have chosen such potential for the Rg_2I_2 system.

Hamilton's equations of motion

$$\partial H/\partial Q_i = -P_i \quad (3)$$

$$\partial H/\partial P_i = Q_i \qquad \text{for } (i=1,2,3,4) \quad (4)$$

are solved numerically using a Runge-Kutta fourth-order integration routine. The Morse parameters for Ar-I interactions were taken from reference(16). Those for Kr-I, Xe-I, He-I, He-He, Ar-Ar, Kr-Kr, and Xe-Xe were taken from references (16),(16),(11),(21),(22), (13), and (23) , respectively. These are given in Table I.

The problem of selecting initial conditions for I_2 in the "unbound complex" was treated by assuming Franck-Condon transitions from the I_2 ground state ($X^1\Sigma$) to the excited ($B^3\pi$) state. The initial vibrational phase of I_2 in the ground electronic state was assigned random initial values by assuming that the I_2 and Rg-I oscillators are uncoupled. The phase selection was made using the method described by Porter, Raff, and Miller (19). The initial phase and momentum along the I_2 bond were assigned values appropriate for the v=0, J=0 state of the ground electronic state with the restriction that the I_2 bond length be greater that the inner turning-point of I_2 in the B state for the specified excitation energy.

The I_2 molecule is then "electronically excited" assuming a vertical transition from the X to the B state. This process is illustrated in Figure 2.

TABLE I

POTENTIAL ENERGY PARAMETERS

	D_j(eV)	R_j^o(a.u.)	α (a.u.$^{-1}$)
$I_2(x^1\Sigma)$ (16)	1.555	5.04	0.98690
$I_2(B^3\pi)$ (16)	0.608871	5.69949	0.93752
He-I (11)	0.0017357	7.55901	0.62442
Ar-I (16)	0.02250	8.9008	0.67204
Kr-I (16)	0.0308	7.9201	0.7576
Xe-I (16)	0.0365	8.3534	0.7183
He-He (21)	0.0008806	5.4217	1.106654
Ar-Ar (22)	0.01223	7.200	0.9234
Kr-Kr (13)	0.1740	7.5609	0.793556
Xe-Xe (23)	0.0237813	8.300	0.78189

The momentum along the $I_2(B^3\pi)$ bond was calculated from the kinetic energy obtained by subtracting the potential energy of I_2 at this internuclear distance from the excitation energy. That is, we obtain the bond momentum from equations (5-8). First, we obtain

(5) $$E_\upsilon = (\upsilon + 1/2)\, h\upsilon_0 - (h^2\upsilon_0^2/4D)\,(\upsilon + 1/2)^2$$

as the ground-state energy for the Morse oscillator, I_2. We then electronically excite I_2 and calculate the momentum along the I_2 $B^3\pi$ bond.

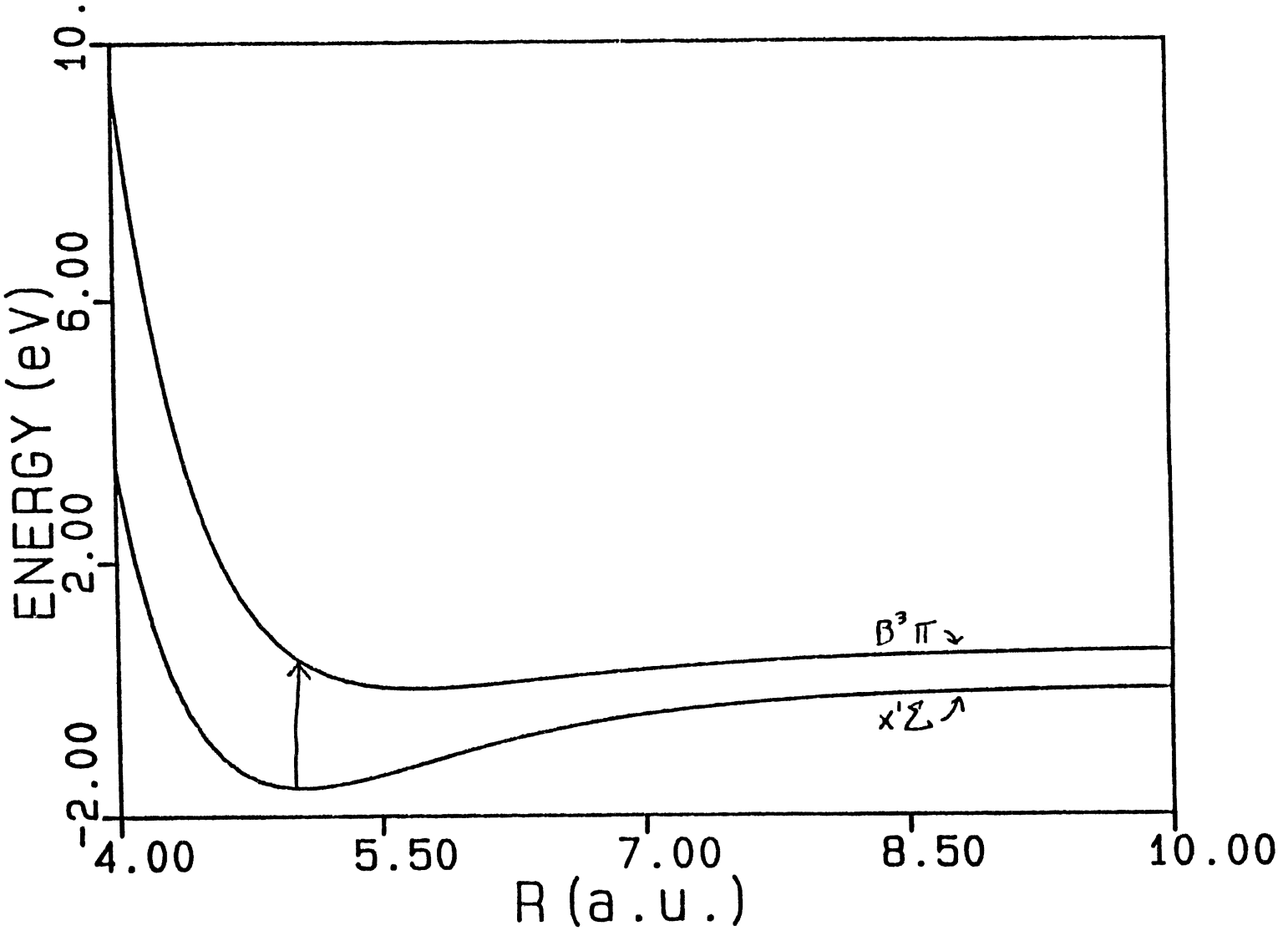

Figure 2. Transition from the $X^1\Sigma$ to the $B^3\Pi$ Electronic State.

(6) $$E_{Total} = E_{\upsilon} + E_{Excitation}$$

(7) $$P_I = (m_I (E_{Total} - E_{Potential, I2})^{1/2}$$

(8) $$P_{I'} = - P_I$$

Equations (5-8) simulate the experimental process as closely as possible. The vibrational energy of the RgI bonds was selected from a Boltzmann distribution at T = 300K, such that the energy was less that the van der Waals well-depth for the T-shaped configuration. This selection is achieved by taking

(9) $$E_{VDW} = -kT \log(1- \xi)$$

where ξ is a randomly chosen number whose distribution is is uniform on the interval [0,1].

The initial value of R was selected randomly within the inner and outer turning-points for the van der Waals bond at the energy given by Eq. (6). The momentum along the van der Waals bond is

(10) $$P_R = \pm \{2\mu_{RgI2}[E - V_{RgI} - V_{RgI'}]\}^{1/2} .$$

where the sign of P_R is selected randomly.

The final state of the individual trajectories was determined by energy and distance criteria. Integration was terminated if either R(the I_2 internuclear distance) or the internuclear distances I_2-Ar or I_2-Ar' became greater than 25 a.u. If R was greater than this value, the internal energy of I_2 was calculated and compared to its dissociation energy. Similar criteria were used to test for the formation of other products. If a trajectory did not

meet these criteria within 4.04 x 10^{-11} s, it was terminated. This time limit in the integration is such that more that 95% of the trajectories dissociated.

The numerical integration was done using a fourth-order Runge-Kutta-Gill routine with a fixed step size of 1.08 x 10^{-14} s. Integration was checked by back-integration and energy conservation. Conservation was to four significant digits.

CHAPTER III

RESULTS AND DISCUSSION

Calculations were carried out a four different initial excitation energies of I_2 for each complex: 0.609, 0.620, 0.640, and 0.660 eV. All of these are above the $I_2(B^3\pi)$ dissociation energy (0.608871 eV). Five hundred trajectories were computed at each energy. The eight possible dissociation channels for Rg_2I_2 are as follows:

$$Rg_2I_2 \xrightarrow{k_1} I_2 + Rg + Rg' \qquad \text{Channel 1}$$

$$\xrightarrow{k_2} 2I + Rg + Rg' \qquad \text{Channel 2}$$

$$\xrightarrow{k_3} I[2] + Rg[2] \qquad \text{Channel 3}$$

$$\xrightarrow{k_4} RgI_2 + Rg \qquad \text{Channel 4}$$

$$Rg'I_2 + Rg$$

$$\xrightarrow{k_5} Rg_2I + I' \qquad \text{Channel 5}$$

$$Rg[2]I' + I$$

k_6

----------> $RgI + Rg' + I'$ Channel 6

$Rg'I + Rg + I'$

$RgI' + I + Rg'$

$Rg'I' + Rg + I$

k_7

----------> $IRg + I'Rg'$ Channel 7

$IRg' + I'Rg$

k_8

----------> $Rg_2 + I + I'$ Channel 8

k_9

----------> Rg_2I_2 Channel 9

The number of products formed in each channel is presented in Table I. While product numbers are useful data, it is desirable to present the data in a form compatible to that available by experiment. This is accomplished by extracting individual rate coefficients for the respective reaction channels. The individual rate coefficients are given by

(11) $$k_n = k_{total}\, Pn / (P_1 + P_2 + ... + P_8)$$

where k_{total} is the overall rate coefficient. The values of the k_i and k_{total} for each rare gas are also given in Tables II-V. After it was determined that a trajectory had dissociated, its lifetime was taken as the trajectory time at the last encounter of the inner turning point just

prior to the escape of Rg. The distribution of lifetimes obtained by this procedure was fit (by least squares) to

(12) $\ln(N_t/N_o) = - kt$

where N_o is the total number of trajectories in the ensemble, N_t is the number of nondissociated trajectories at time t, and k is the decay rate coefficient. These are plotted in Figures 3-16.

TABLE II

RARE GAS = ARGON

A. PRODUCT NUMBERS

CHAN	EEX=0.609 eV	EEX=0.620 eV	EEX=0.640 eV	EEX=0.660 eV
1	40	53	37	38
2	0	0	0	0
3	27	18	16	11
4	417	402	371	309
5	14	18	45	67
6	1	2	14	57
7	1	7	17	42
8	0	0	0	0

B. OVERALL RATE COEFFICIENTS

	EEX(eV)	RATE COEFFICIENT (sec^{-1})
1	0.60900	0.1271413D+12
2	0.62000	0.9709121D+11
3	0.64000	0.1075882D+12
4	0.66000	0.1270861D+12

TABLE II (Continued)

C. INDIVIDUAL RATE COEFFICIENTS (SEC^{-1})

CHAN	EEX=0.609 eV	EEX=0.620 eV	EEX=0.640 eV	EEX=0.660 eV
1	0.91581D+10	0.10292D+11	0.79615D+10	0.91811D+10
2	0.00000D+00	0.00000D+00	0.00000D+00	0.00000D+00
3	0.61817D+10	0.34953D+10	0.34428D+10	0.26577D+10
4	0.95474D+11	0.78061D+11	0.79830D+11	0.74657D+11
5	0.32053D+10	0.34953D+10	0.96829D+10	0.16188D+11
6	0.22895D+09	0.38836D+09	0.30125D+10	0.13772D+11
7	0.22895D+09	0.13593D+10	0.36580D+10	0.10148D+11
8	0.00000D+00	0.00000D+00	0.00000D+00	0.48322D+09
9	0.00000D+00	0.00000D+00	0.00000D+00	0.00000D+00

TABLE III

RARE GAS = KRYPTON

A. PRODUCT NUMBERS

CHAN	EEX=0.609 eV	EEX=0.620 eV	EEX=0.640 eV	EEX=0.660 eV
1	82	66	63	65
2	0	0	0	
3	56	46	37	0
4	351	379	362	311
5	8	7	30	49
6	0	0	1	8
7	3	2	7	26
8	0	0	0	1
9	0	0	0	0

B. OVERALL RATE COEFFICIENTS

	EEX(eV)	RATE COEFFICIENT (sec^{-1})
1	0.60900	0.1967445D+12
2	0.62000	0.1803352D+12
3	0.64000	0.1668728D+12
4	0.66000	0.1504544D+12

TABLE III (Continued)

C. INDIVIDUAL RATE COEFFICIENTS (SEC^{-1})

CHAN	EEX=0.609 eV	EEX=0.620 eV	EEX=0.640 eV	EEX=0.660 eV
1	0.32266D+11	0.23804D+11	0.21026D+11	0.19559D+11
2	0.00000D+00	0.00000D+00	0.00000D+00	0.00000D+00
3	0.22035D+11	0.16591D+11	0.12349D+11	0.12036D+11
4	0.13811D+12	0.13669D+12	0.12082D+12	0.93583D+11
5	0.31479D+10	0.25247D+10	0.10012D+11	0.14745D+11
6	0.00000D+00	0.00000D+00	0.33375D+09	0.24073D+10
7	0.11805D+10	0.72134D+09	0.23362D+10	0.78236D+10
8	0.00000D+00	0.00000D+00	0.00000D+00	0.30091D+09
9	0.00000D+00	0.00000D+00	0.00000D+00	0.00000D+00

TABLE IV

RARE GAS = XENON

A. PRODUCT NUMBERS

CHAN	EEX=0.609 eV	EEX=0.620 eV	EEX=0.640 eV	EEX=0.660 eV
1	64	61	50	59
2	0	0	0	0
3	61	53	76	62
4	372	369	342	305
5	3	17	23	45
6	0	0	1	7
7	0	0	8	21
8	0	0	0	1
9	0	0	0	0

B. OVERALL RATE COEFFICIENTS

	EEX(eV)	RATE COEFFICIENT (sec^{-1})
1	0.60900	0.1591159D+12
2	0.62000	0.1480265D+12
3	0.64000	0.1476768D+12
4	0.66000	0.1320269D+12

TABLE IV (Continued)

C. INDIVIDUAL RATE COEFFICIENTS (SEC^{-1})

CHAN	EEX=0.609 eV	EEX=0.620 eV	EEX=0.640 eV	EEX=0.660 eV
1	0.20367D+11	0.18059D+11	0.14768D+11	0.15579D+11
2	0.00000D+00	0.00000D+00	0.00000D+00	0.00000D+00
3	0.19412D+11	0.15691D+11	0.22447D+11	0.16371D+11
4	0.11838D+12	0.10924D+12	0.10101D+12	0.80536D+11
5	0.95470D+09	0.50329D+10	0.67931D+10	0.11882D+11
6	0.00000D+00	0.00000D+00	0.29535D+09	0.18484D+10
7	0.00000D+00	0.00000D+00	0.23628D+10	0.55451D+10
8	0.00000D+00	0.00000D+00	0.00000D+00	0.26405D+09
9	0.00000D+00	0.00000D+00	0.00000D+00	0.00000D+00

TABLE V

RARE GAS = HELIUM

A. PRODUCT NUMBERS

CHAN	EEX=0.609 eV
1	0
2	0
3	0
4	0
5	0
6	384
7	0
8	116
9	0

TABLE V (Continued)

B. OVERALL RATE COEFFICIENTS

	EEX(eV)	RATE COEFFICIENT (sec^{-1})
1	0.60900	0.5220145D+12

C. INDIVIDUAL RATE COEFFICIENTS (SEC^{-1})

CHAN	EEX=0.609 eV
1	0.00000D+00
2	0.00000D+00
3	0.00000D+00
4	0.00000D+00
5	0.00000D+00
6	0.40085D+12
7	0.00000D+00
8	0.12117D+12
9	0.00000D+00

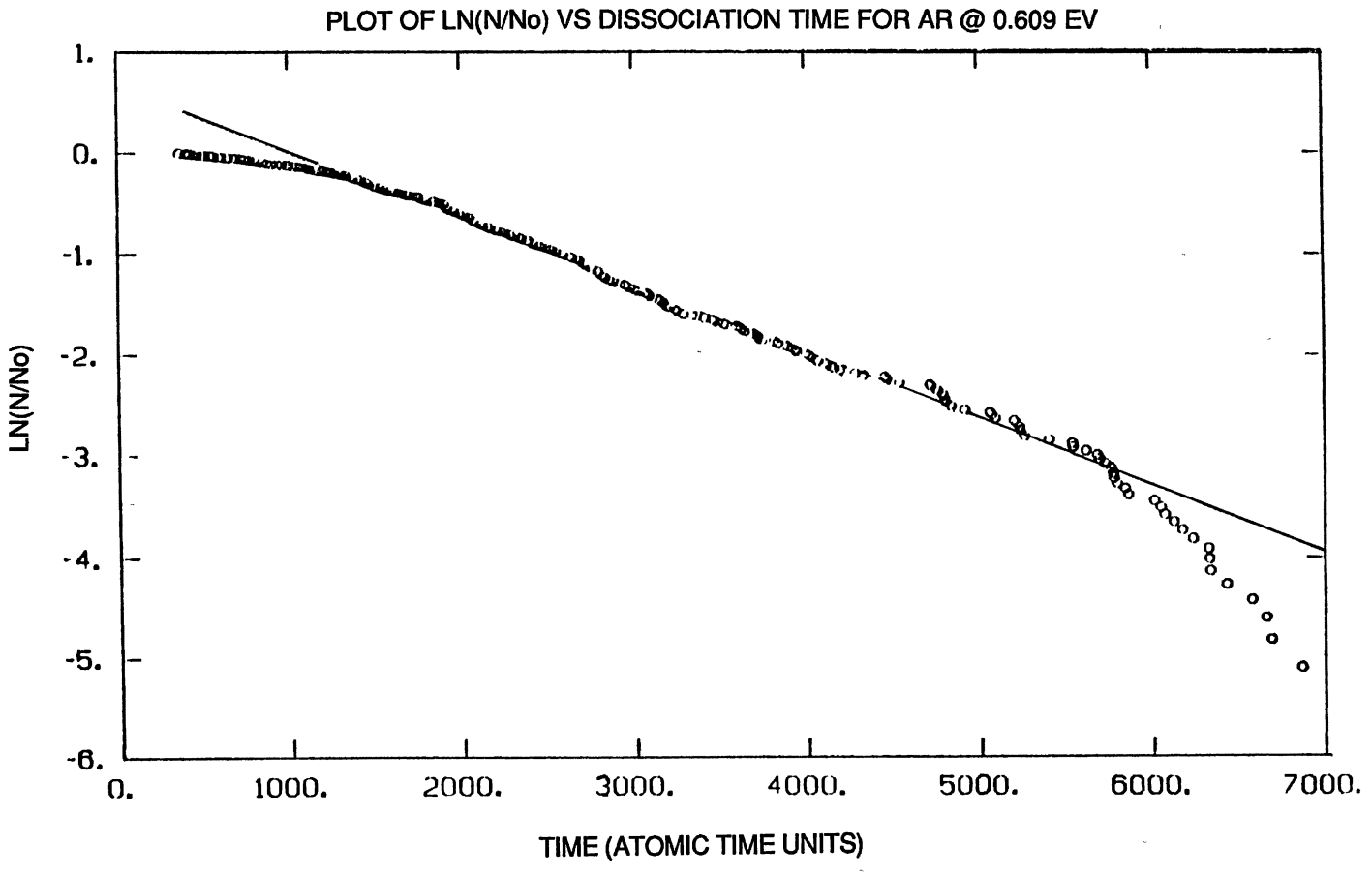

Figure 3. Plot of $\ln(N/N_0)$ vs. Dissociation Time for Ar at 0.609 eV.

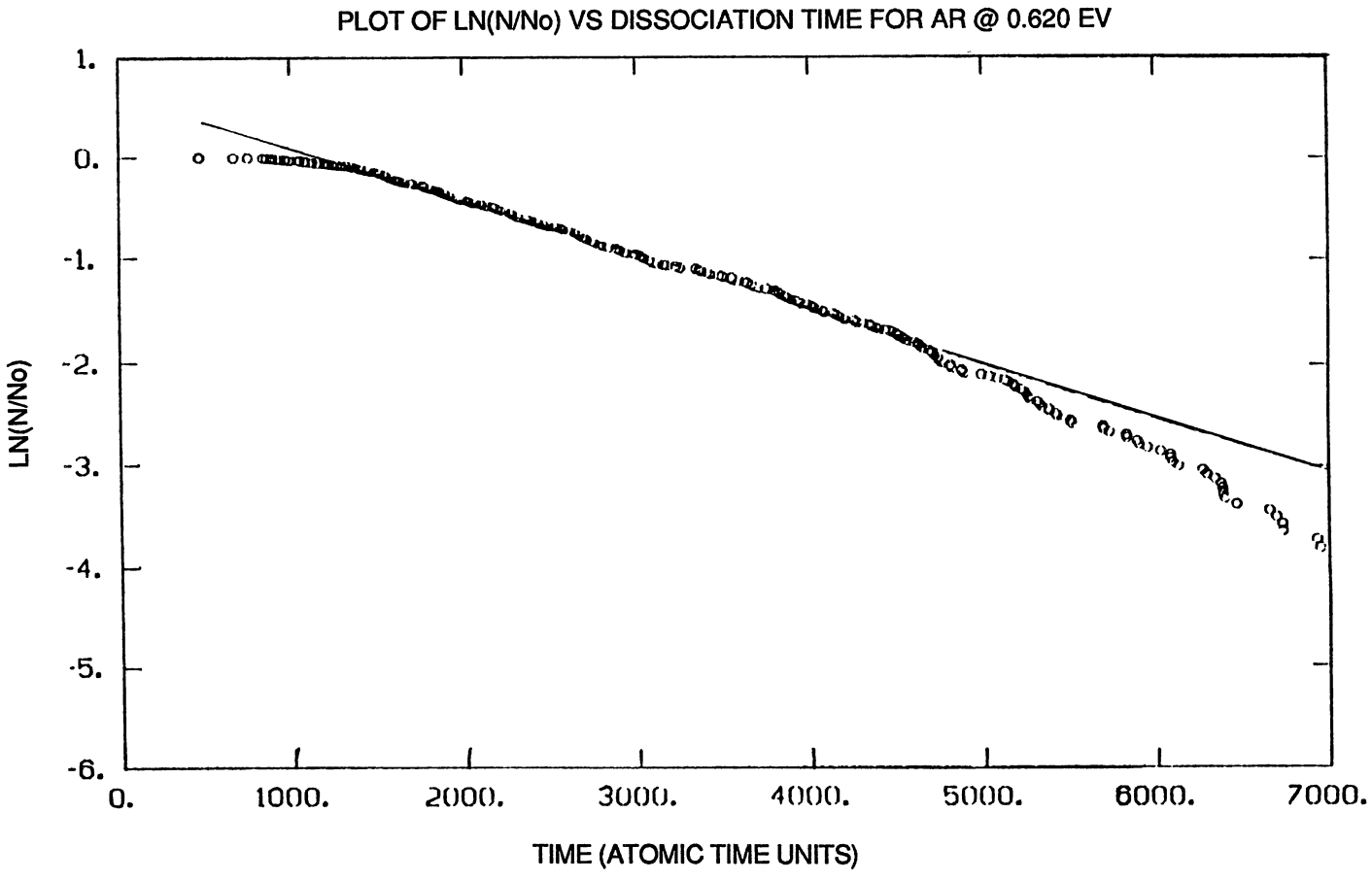

Figure 4. Plot of $\ln(N/N_0)$ vs. Dissociation Time for Ar at 0.620 eV.

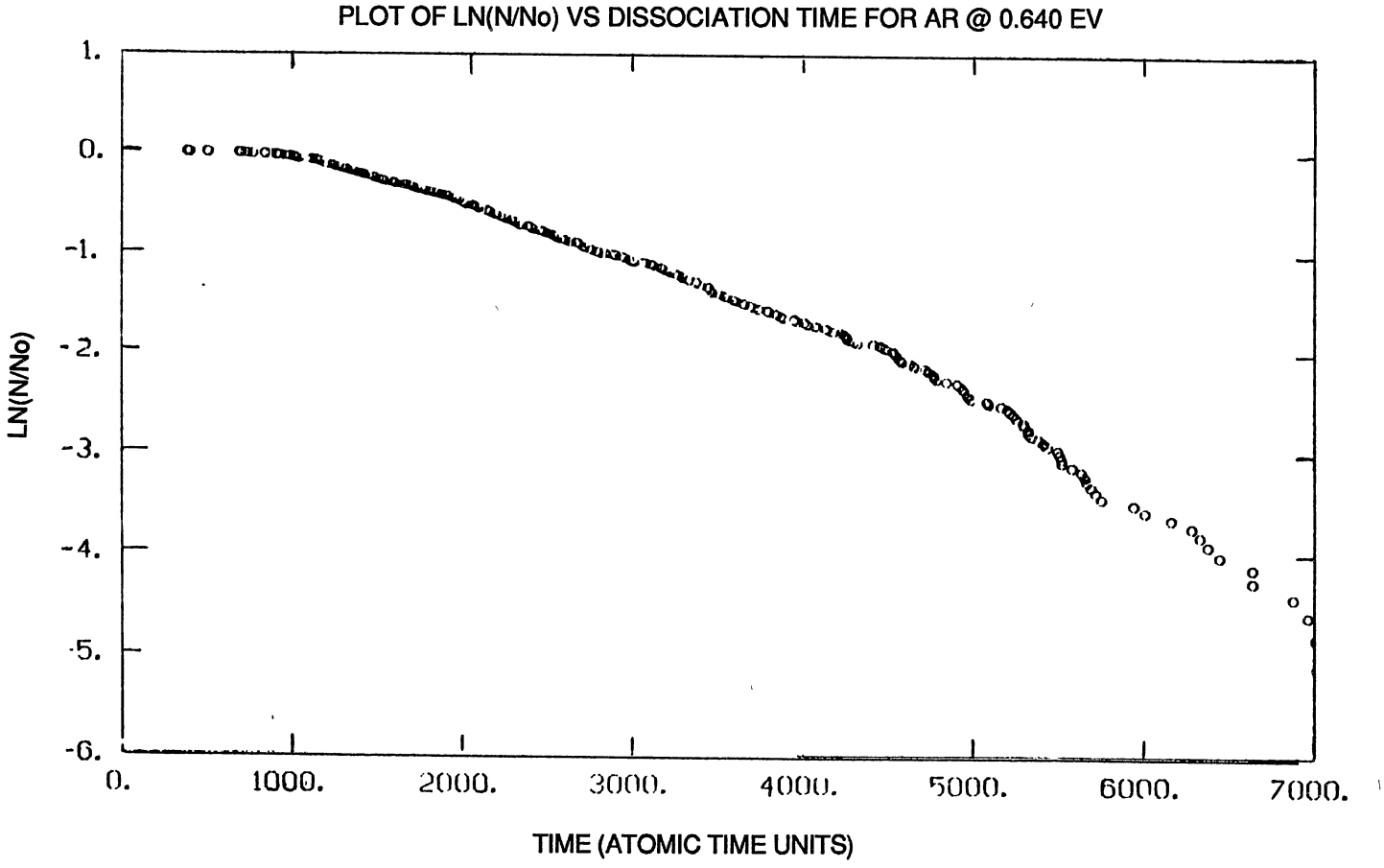

Figure 5. Plot of $\ln(N/N_0)$ vs. Dissociation Time for Ar at 0.640 eV.

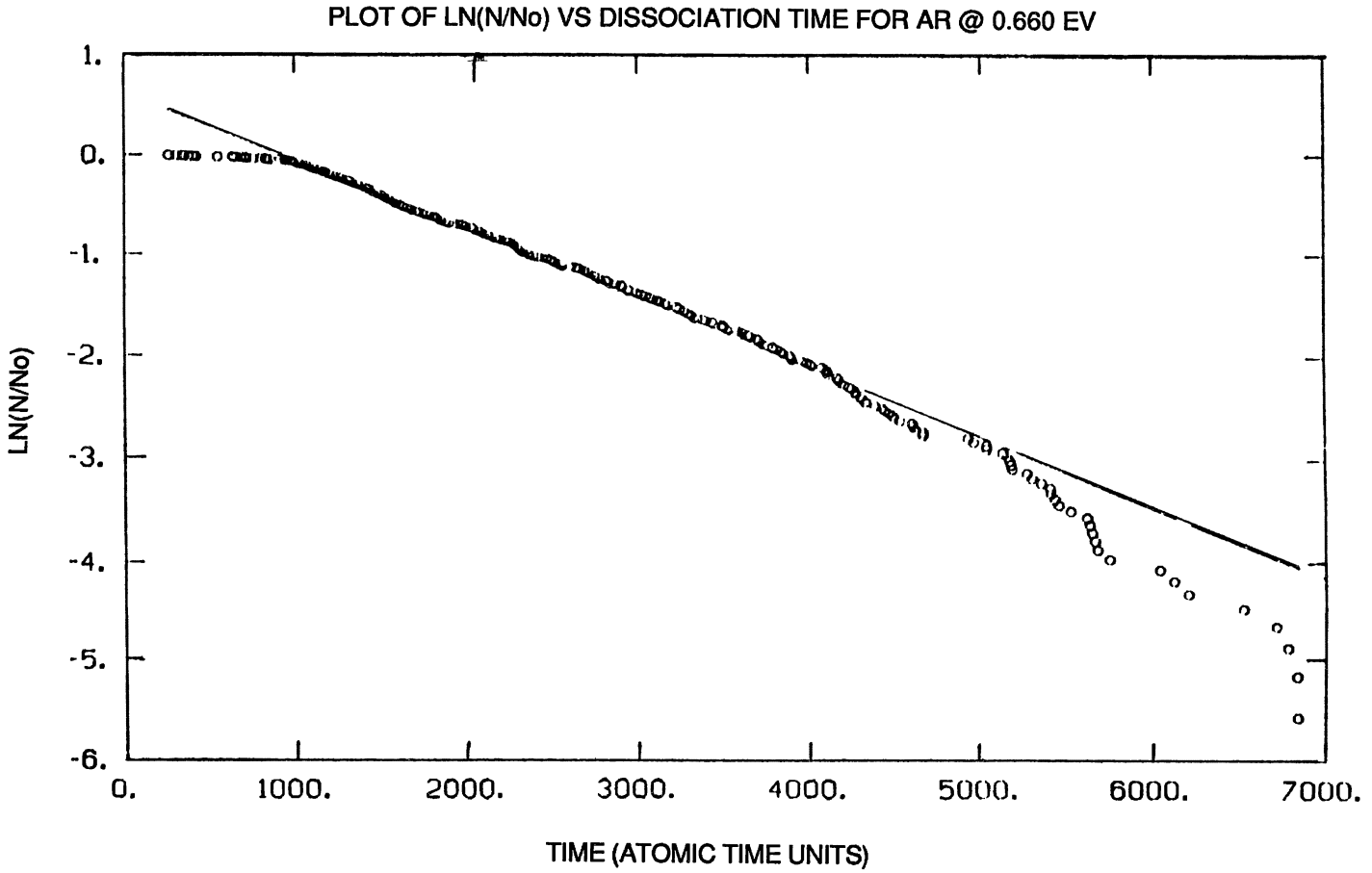

Figure 6. Plot of $\ln(N/N_0)$ vs. Dissociation Time for Ar at 0.660 eV.

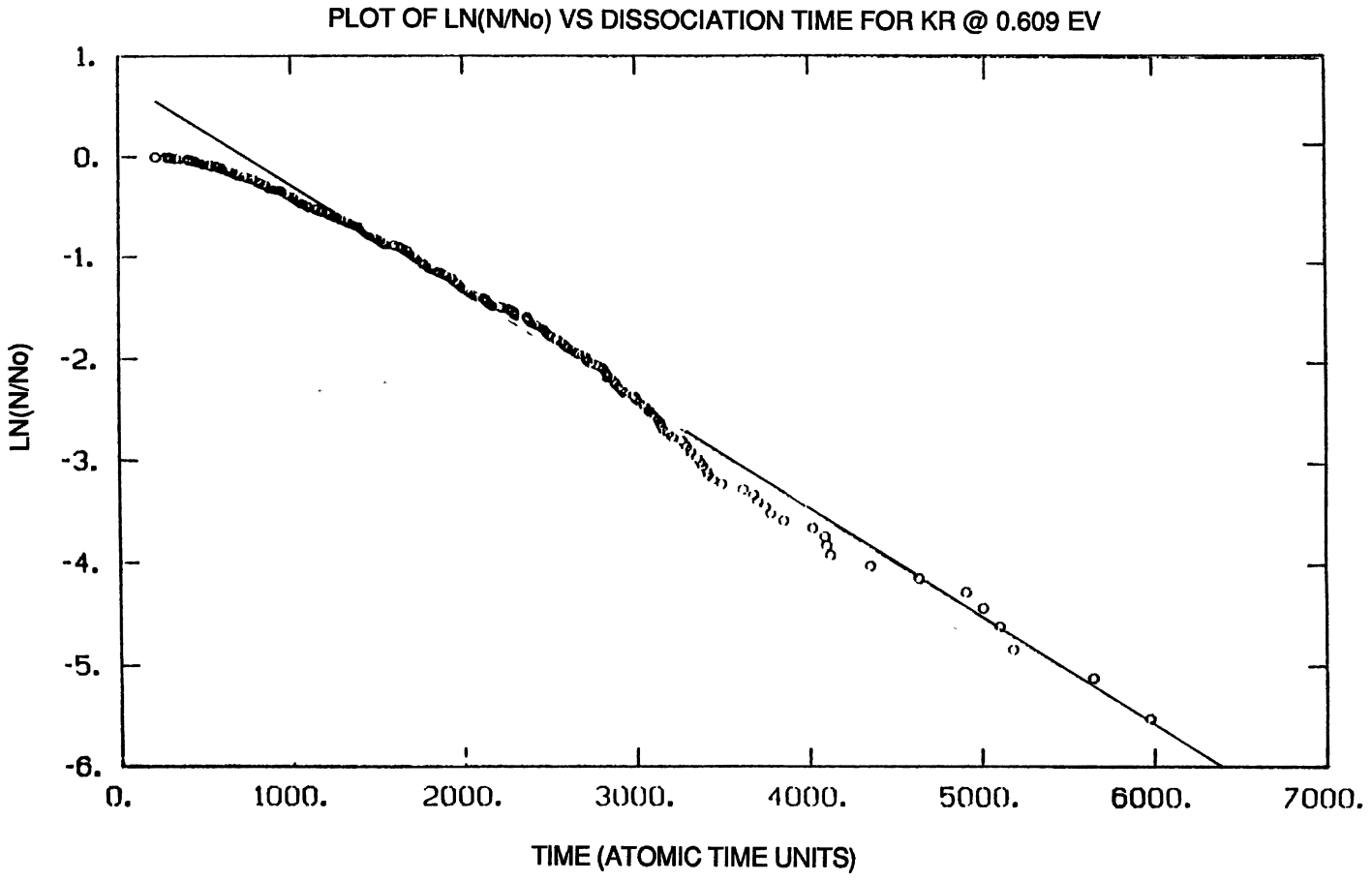

Figure 7. Plot of $\ln(N/N_0)$ vs. Dissociation Time for Kr at 0.609 eV.

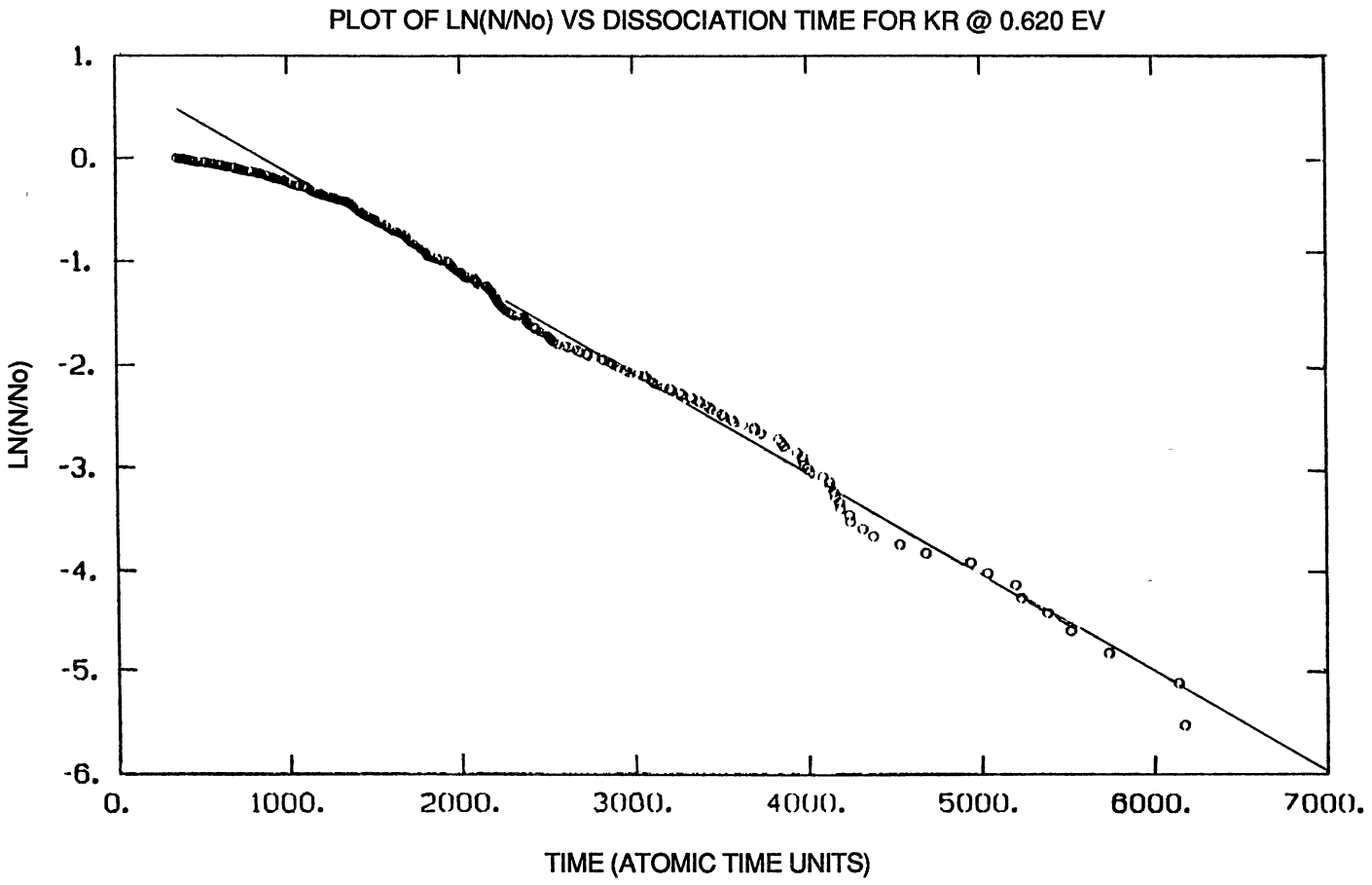

Figure 8. Plot of $\ln(N/N_0)$ vs. Dissociation Time for Kr at 0.620 eV.

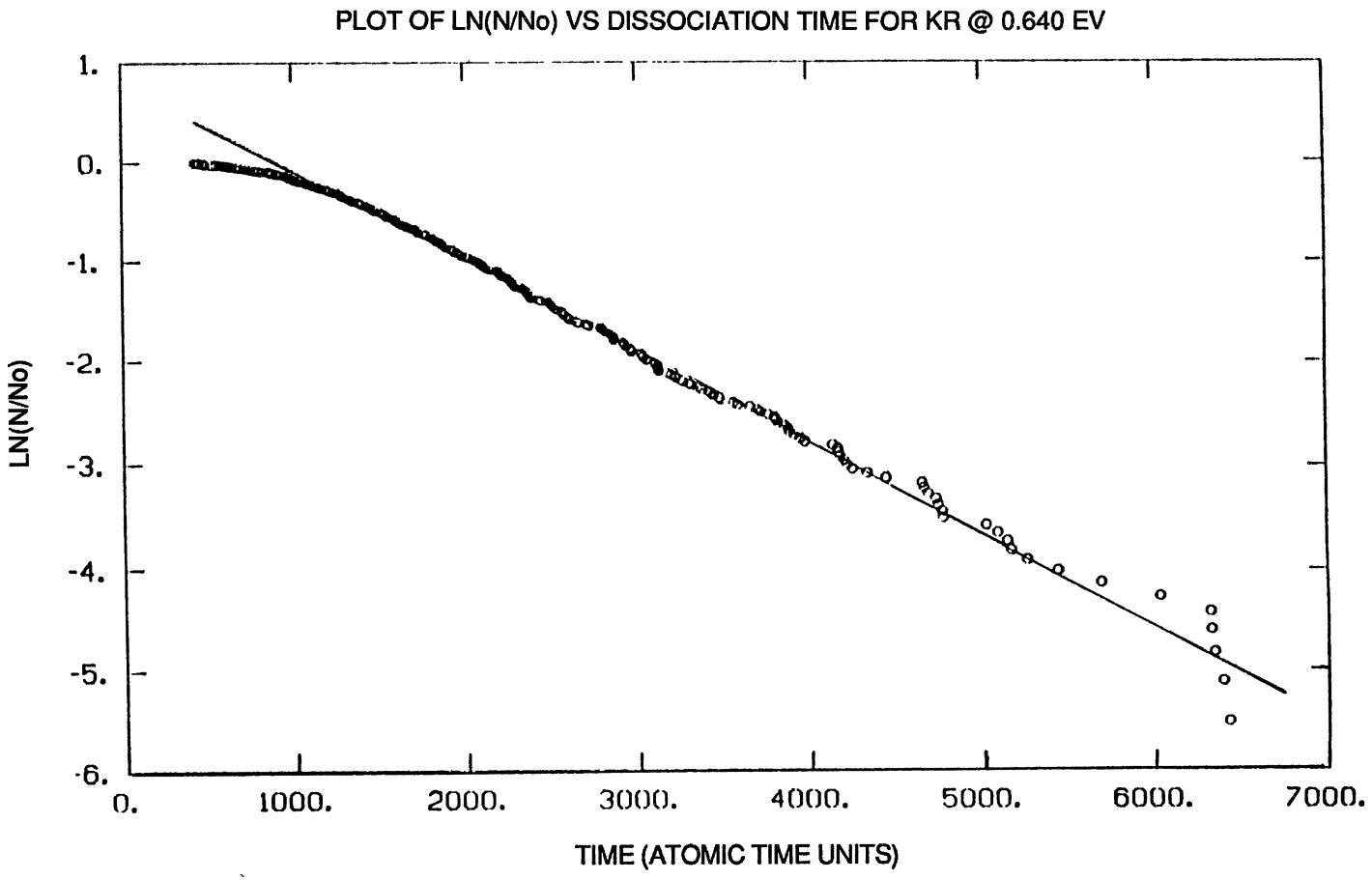

Figure 9. Plot of $\ln(N/N_0)$ vs. Dissociation Time for Kr at 0.640 eV.

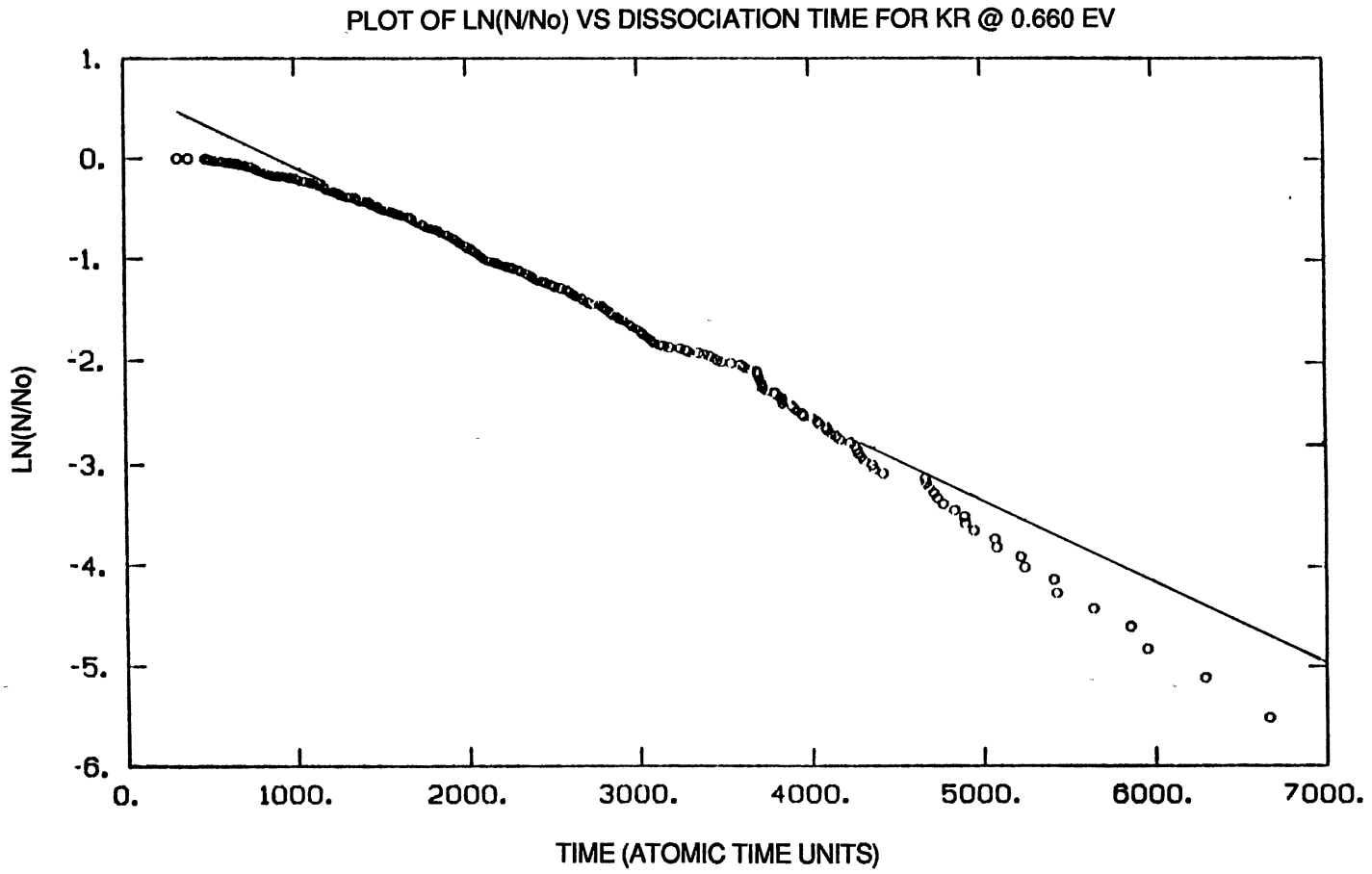

Figure 10. Plot of $\ln(N/N_0)$ vs. Dissociation Time for Kr at 0.660 eV.

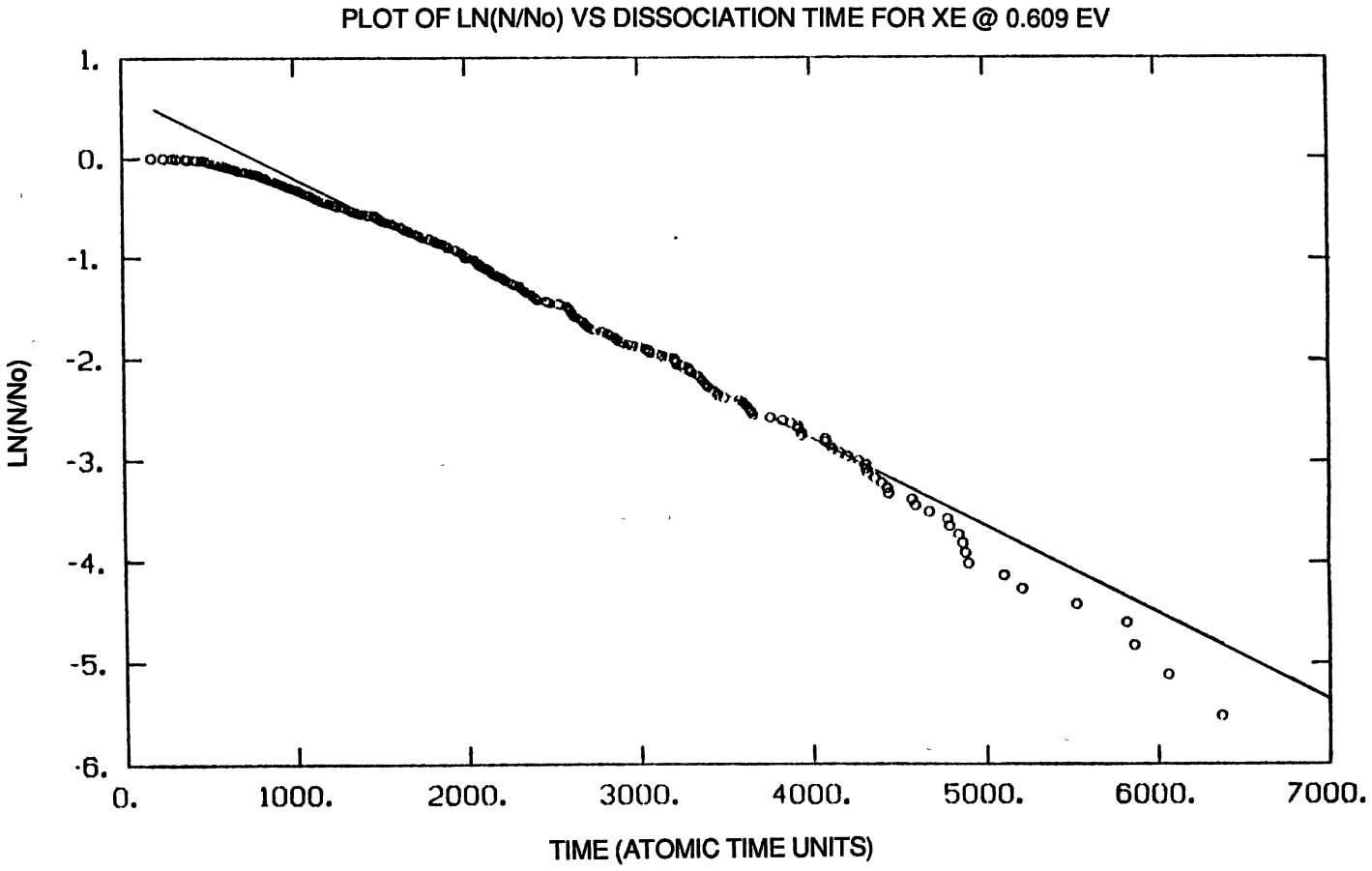

Figure 11. Plot of $\ln(N/N_0)$ vs. Dissociation Time for Xe at 0.609 eV.

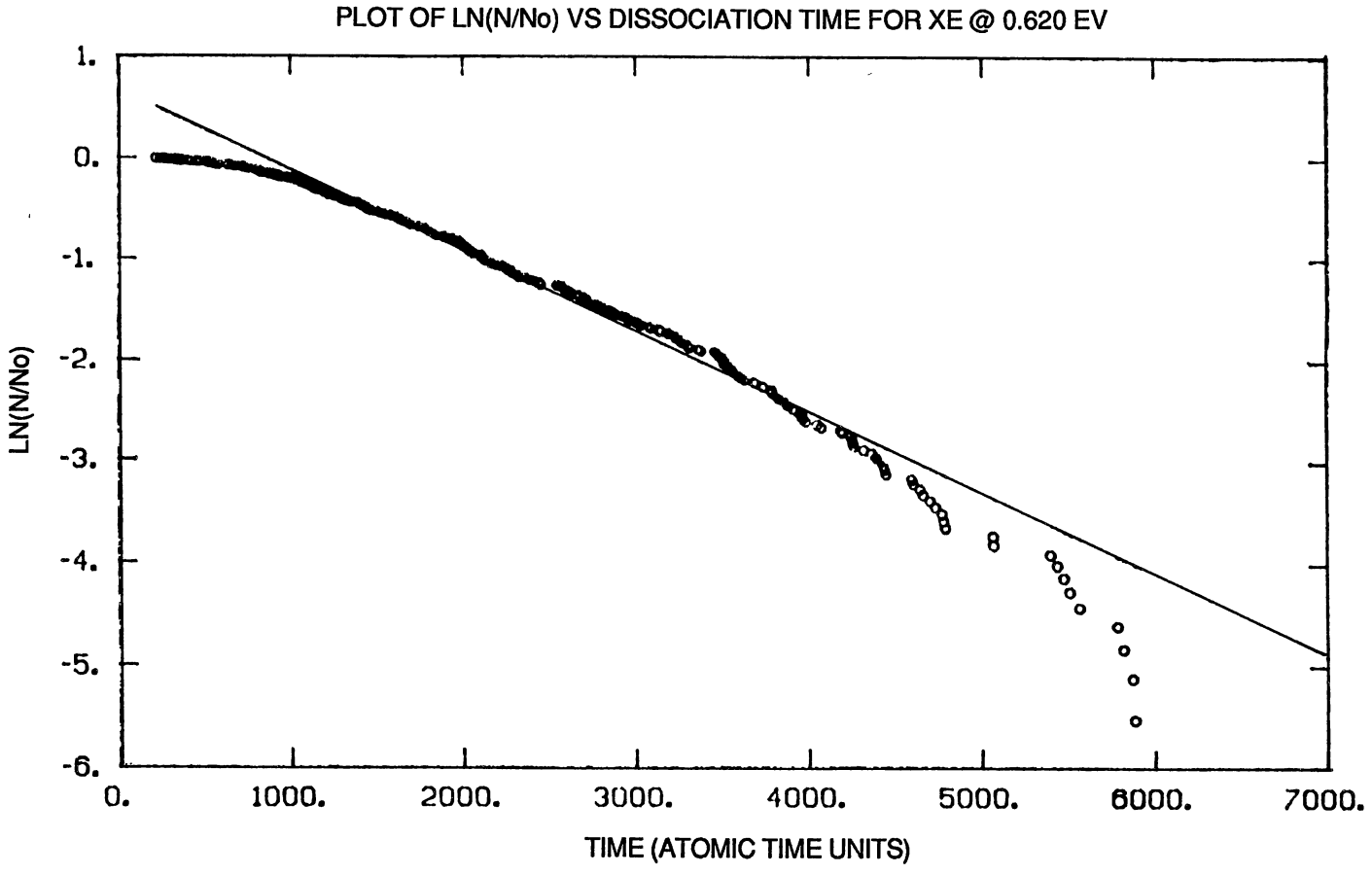

Figure 12. Plot of $\ln(N/N_0)$ vs. Dissociation Time for Xe at 0.620 eV.

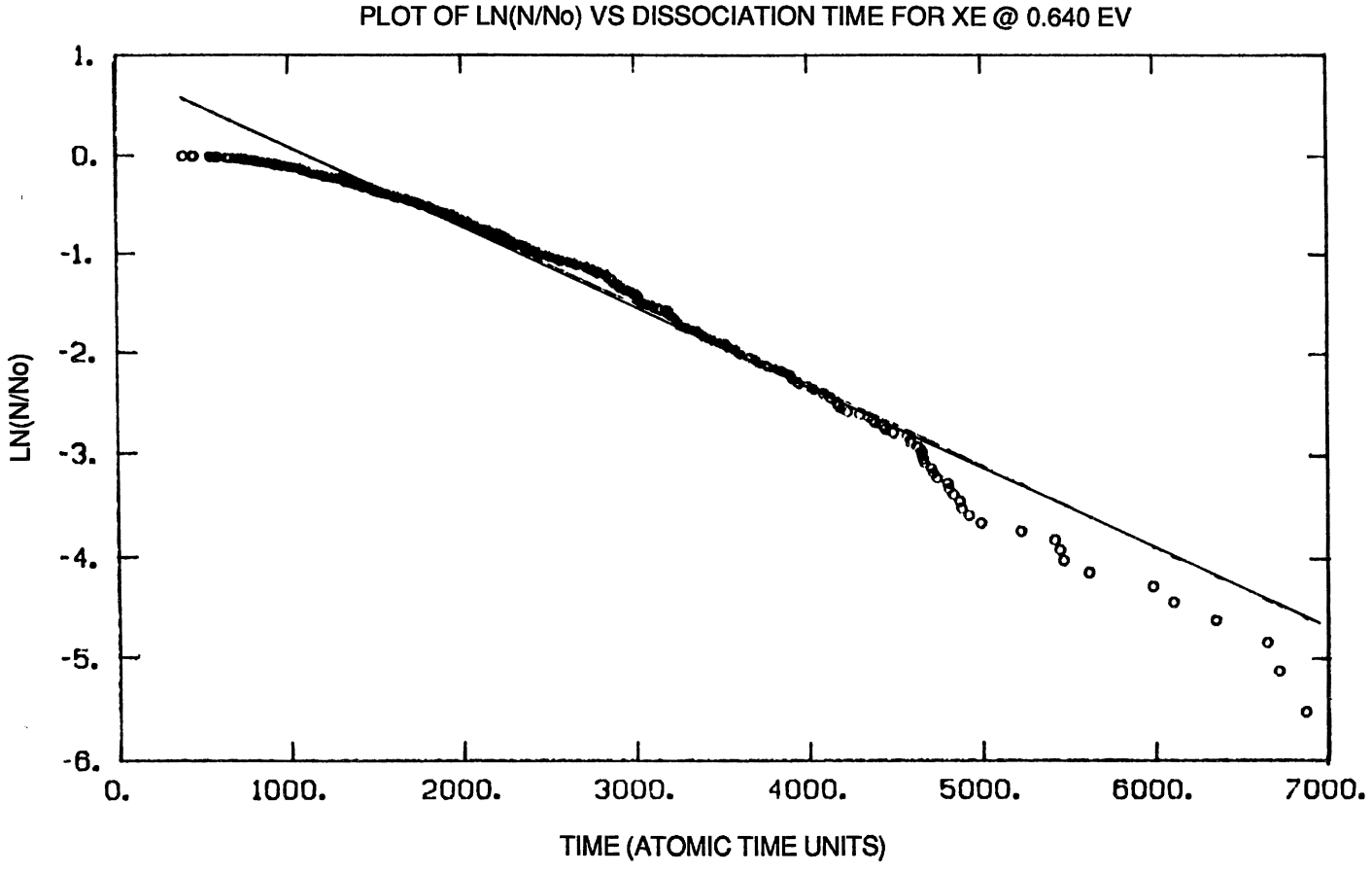

Figure 13. Plot of $\ln(N/N_0)$ vs. Dissociation Time for Xe at 0.640 eV.

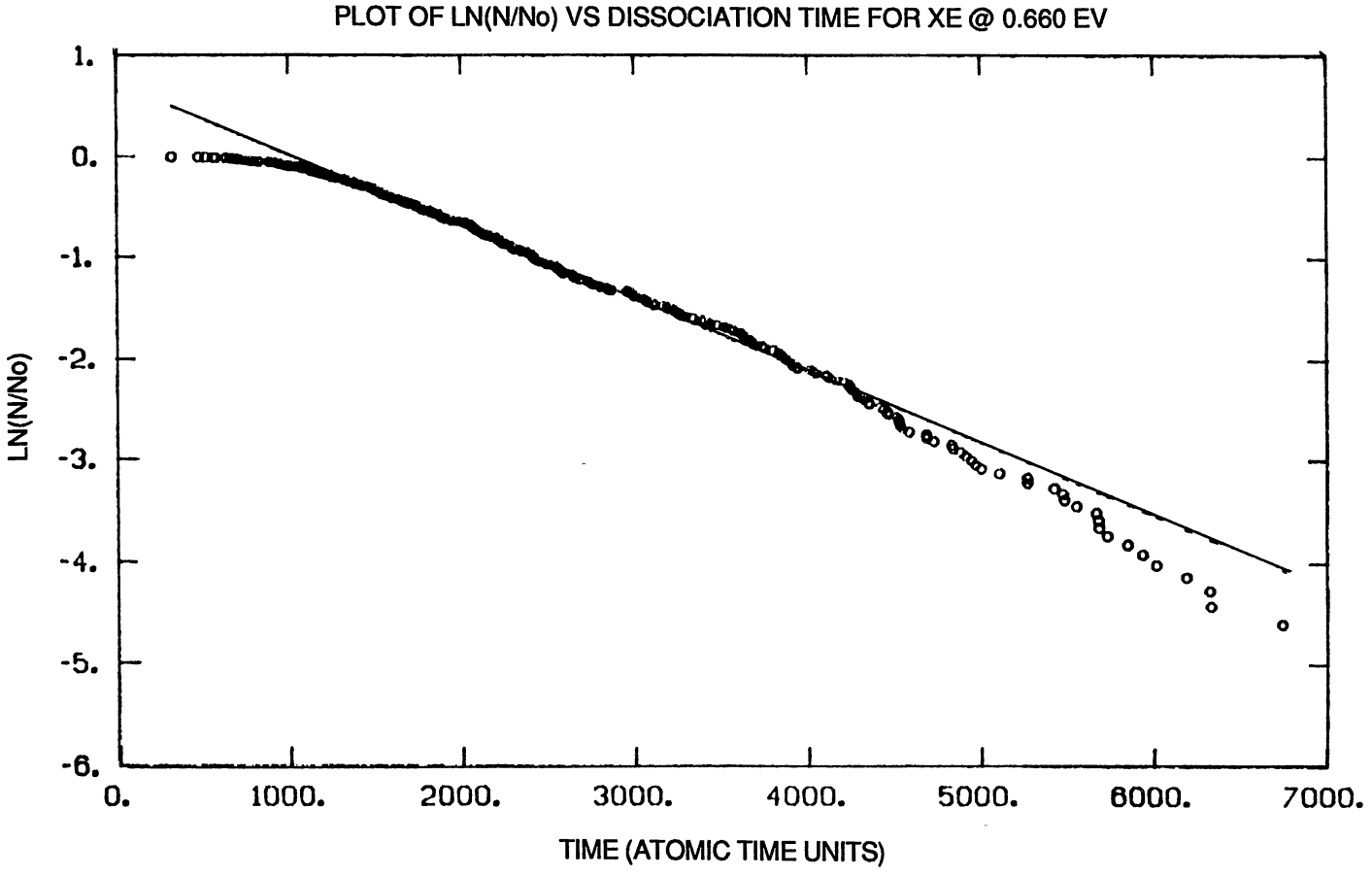

Figure 14. Plot of $\ln(N/N_0)$ vs. Dissociation Time for Xe at 0.660 eV.

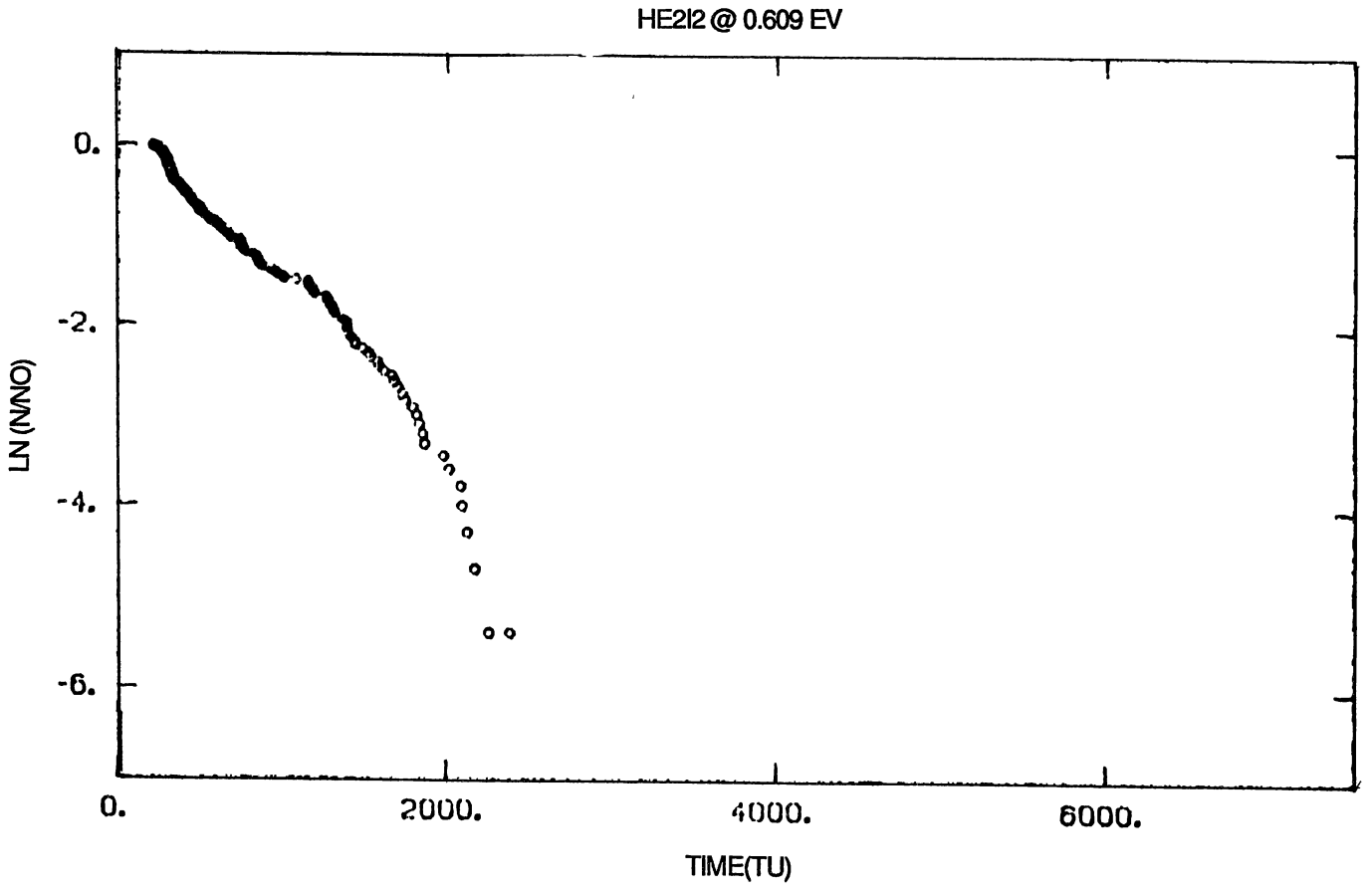

Figure 15. Plot of $\ln(N/N_0)$ vs. Dissociation Time for He at 0.609 eV.

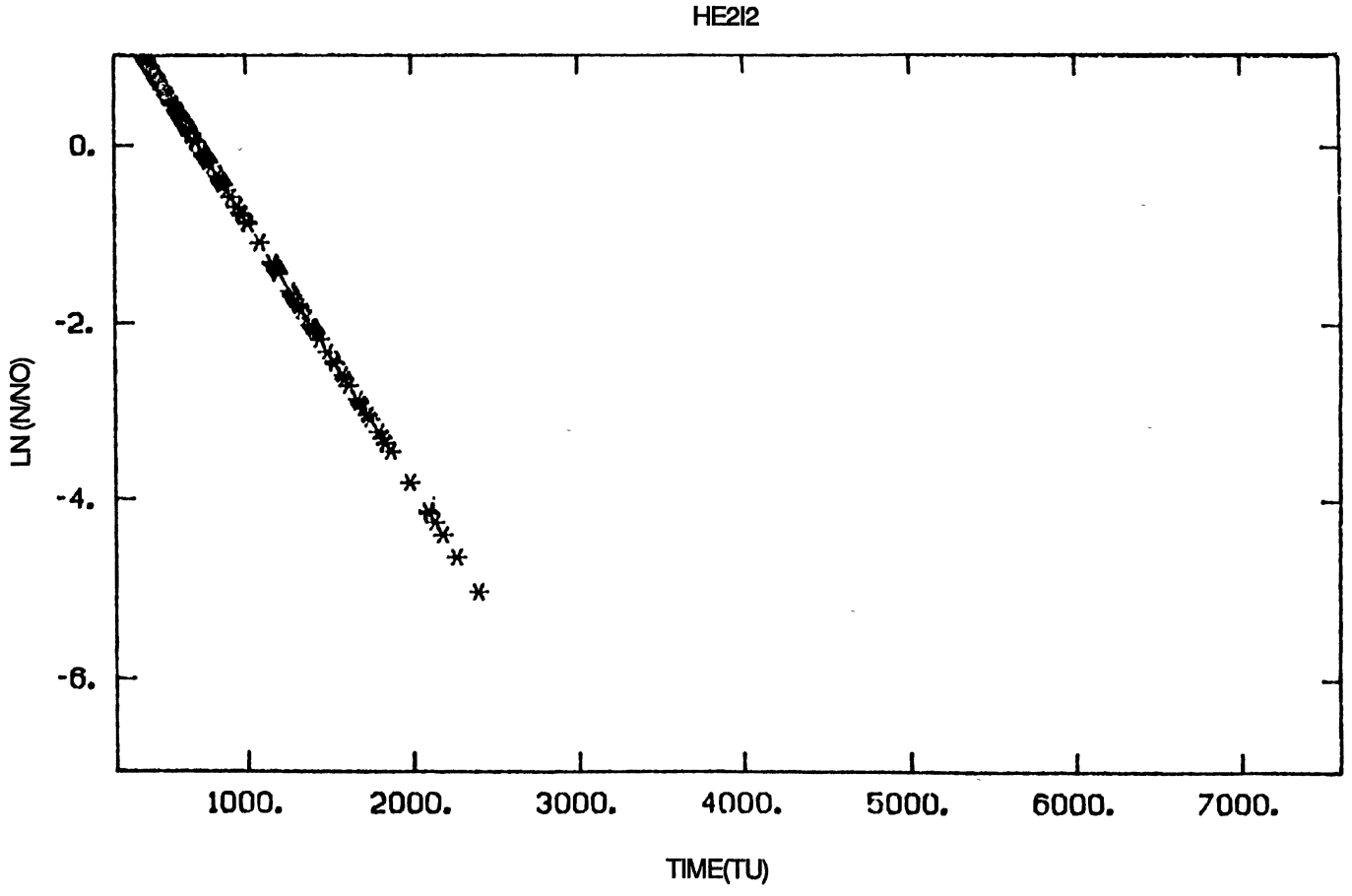

Figure 16. Least-Squares fit for Plot No. 15.

The number of occurrences of product formation as a function of excitation energy are plotted on Figures 17-28, for Ar, Kr, and Xe.

"Most probable" product recoil energies were obtained by fitting the histogrammed data to a Gaussian function. The most probable recoil energy was obtained from the Gaussian fitting parameter. As in Noorbatcha's study (16), a large fraction of I_2 molecules are formed with energy well below the dissociation limit. There is a trend toward lower overall recoil energy, as would be expected with the increased mass available for energy transfer in the four-atom system as opposed to the three- atom system. Also in common with Noorbatcha's study is the linearity of most probable recoil energy with increasing initial excitation energy. The slopes of the straight lines plotted in Figure 29 are 0.665, 0.746, and 0.867 for Ar_2I_2, Kr_2I_2, and Xe_2I_2 respectively.

NoorBatcha obtained 0.84, 1.12, and 1.00 for the analogous three atom systems. The results indicate an orderly progression of increasing energy-transfer efficiency with increasing mass.

Contrary to preliminary results obtained by Philippoz et. al. (18), the dissociation of the He_2I_2 complex was found not to yield molecular I_2 under any circumstances. Trajectories were consequently run using only the lowest excitation energy. Only Channels 6 and 8 were found to be present. Thus the present results show that not only is He less efficient than Ar in energy transfer, but that He is unable to prevent the fragmentation of the excited I_2 into atomic I. Consequently, the source of the I_2 in the Phillipoz' et.al. (18) experiment is uncertain.

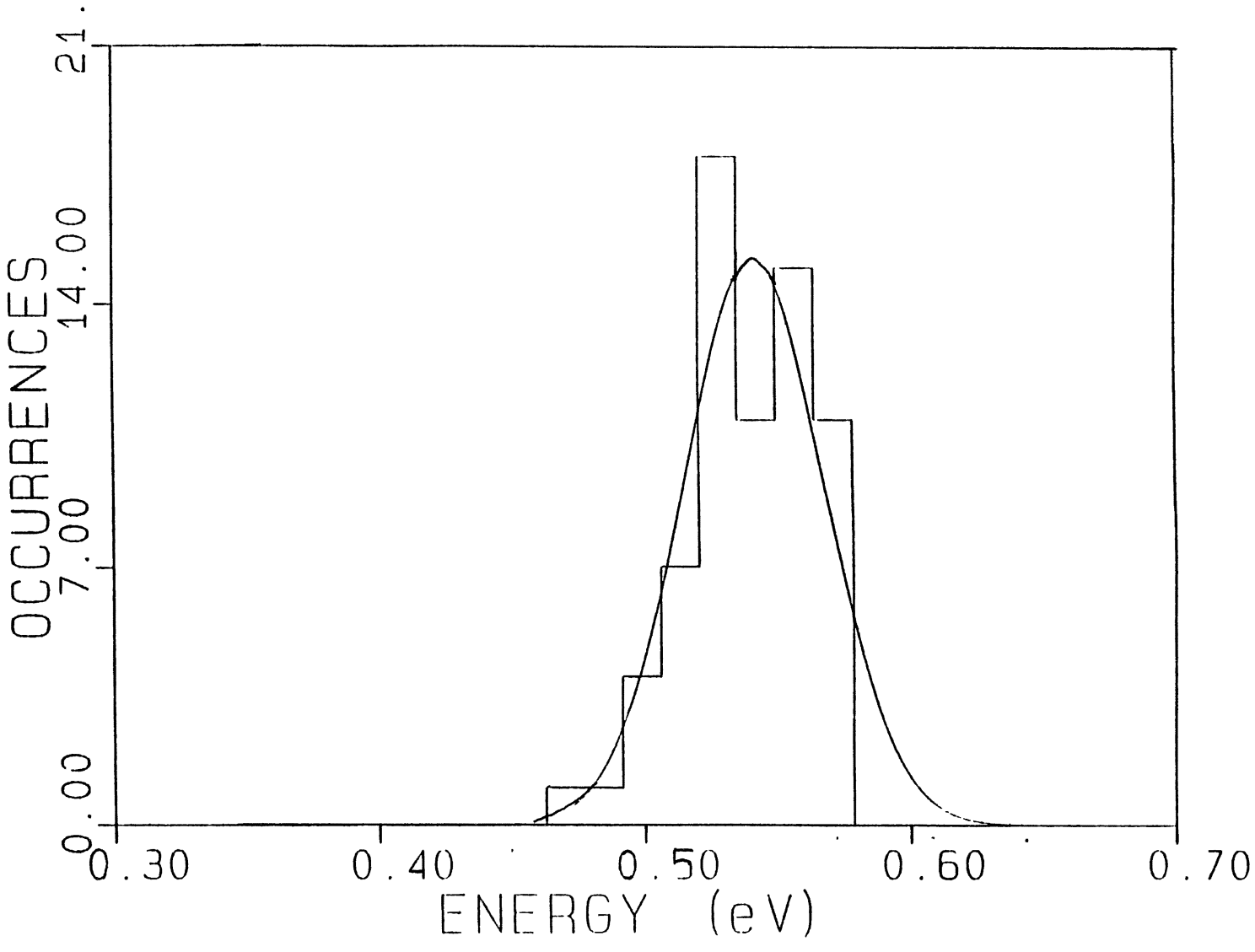

Figure 17. Plot of Number of Occurrences vs. Recoil Energy for Ar at 0.609 eV.

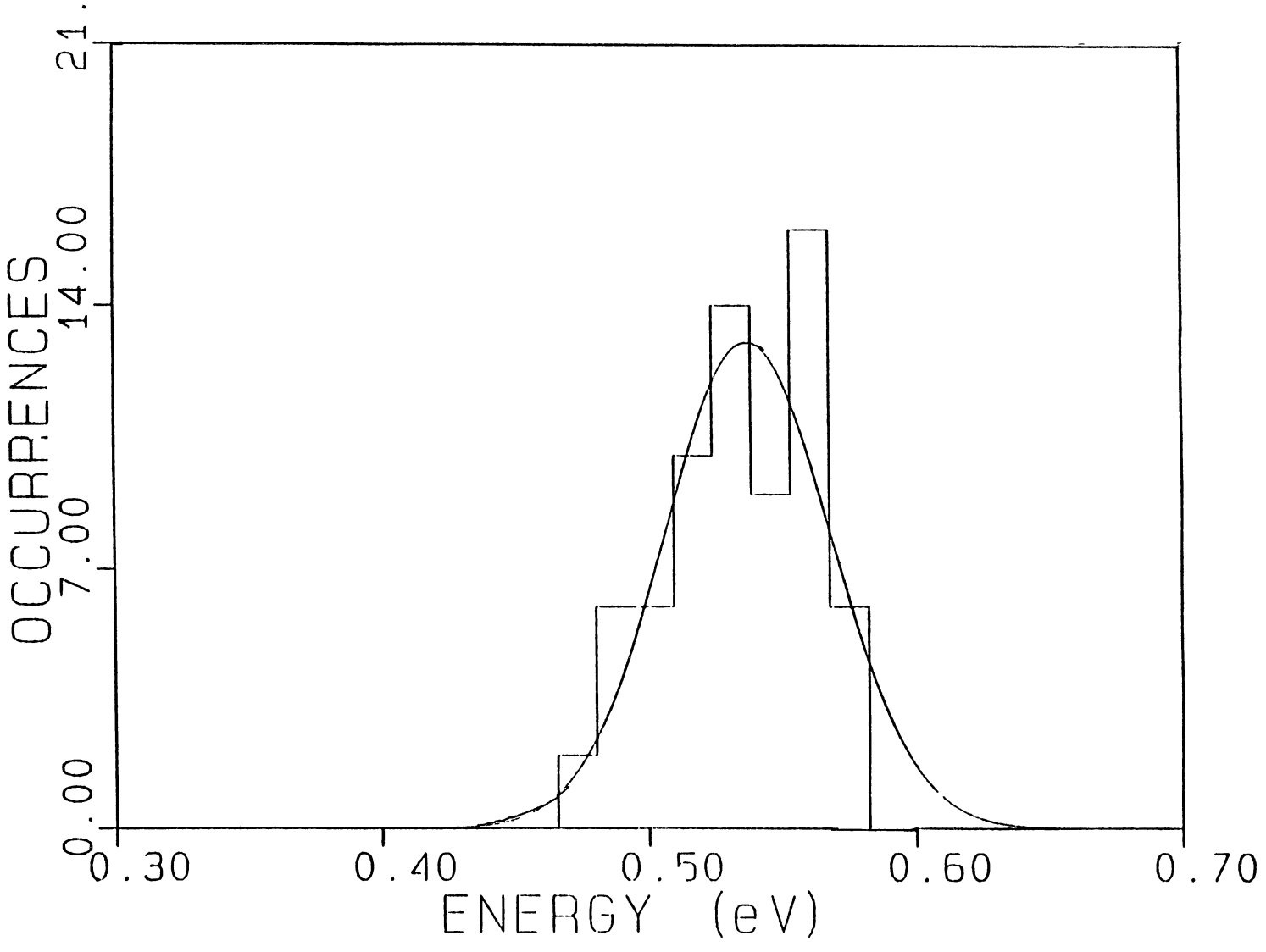

Figure 18. Plot of Number of Occurrences vs. Recoil Energy for Ar at 0.620 eV.

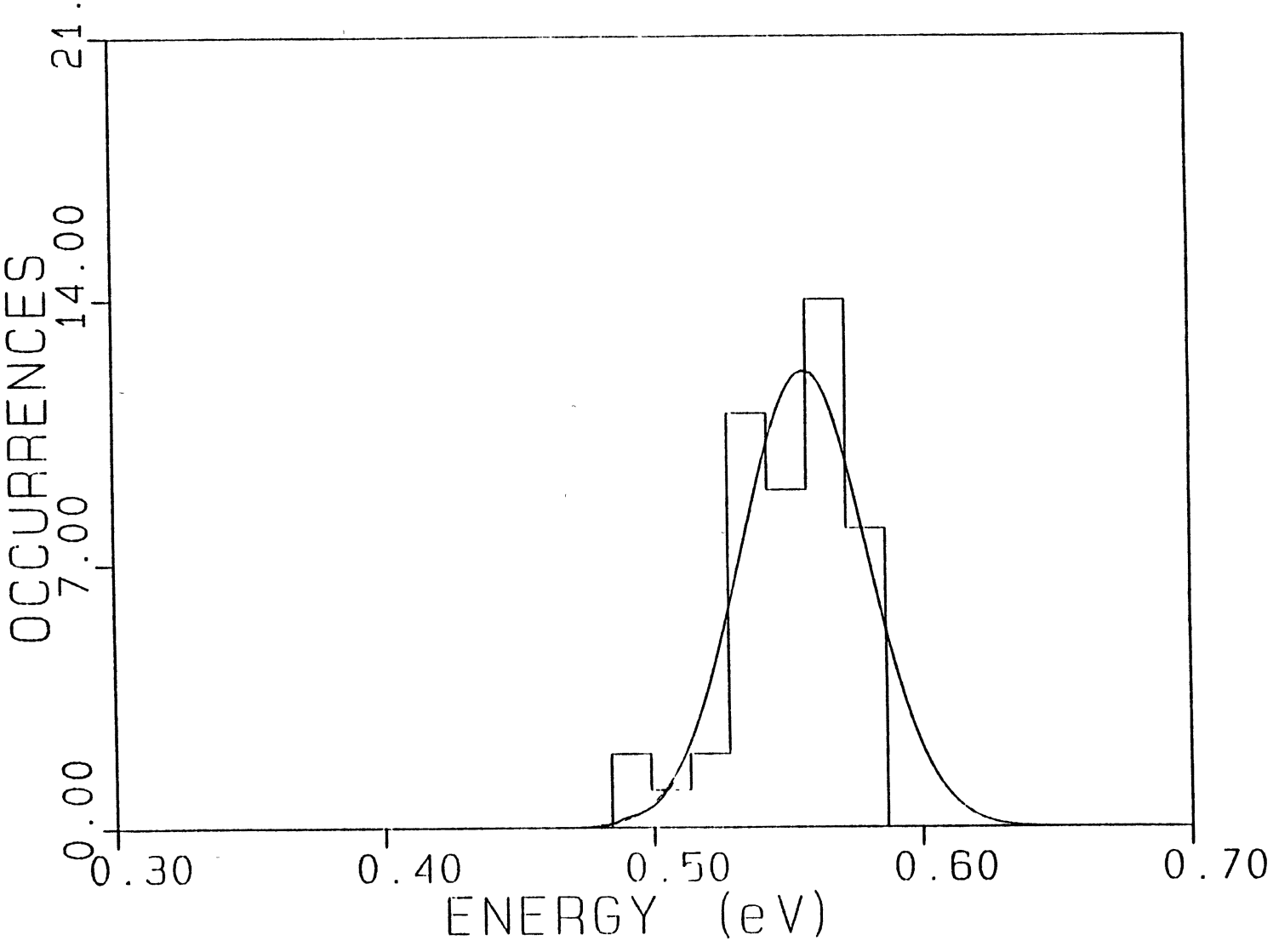

Figure 19. Plot of Number of Occurrences vs. Recoil Energy for Ar at 0.640 eV.

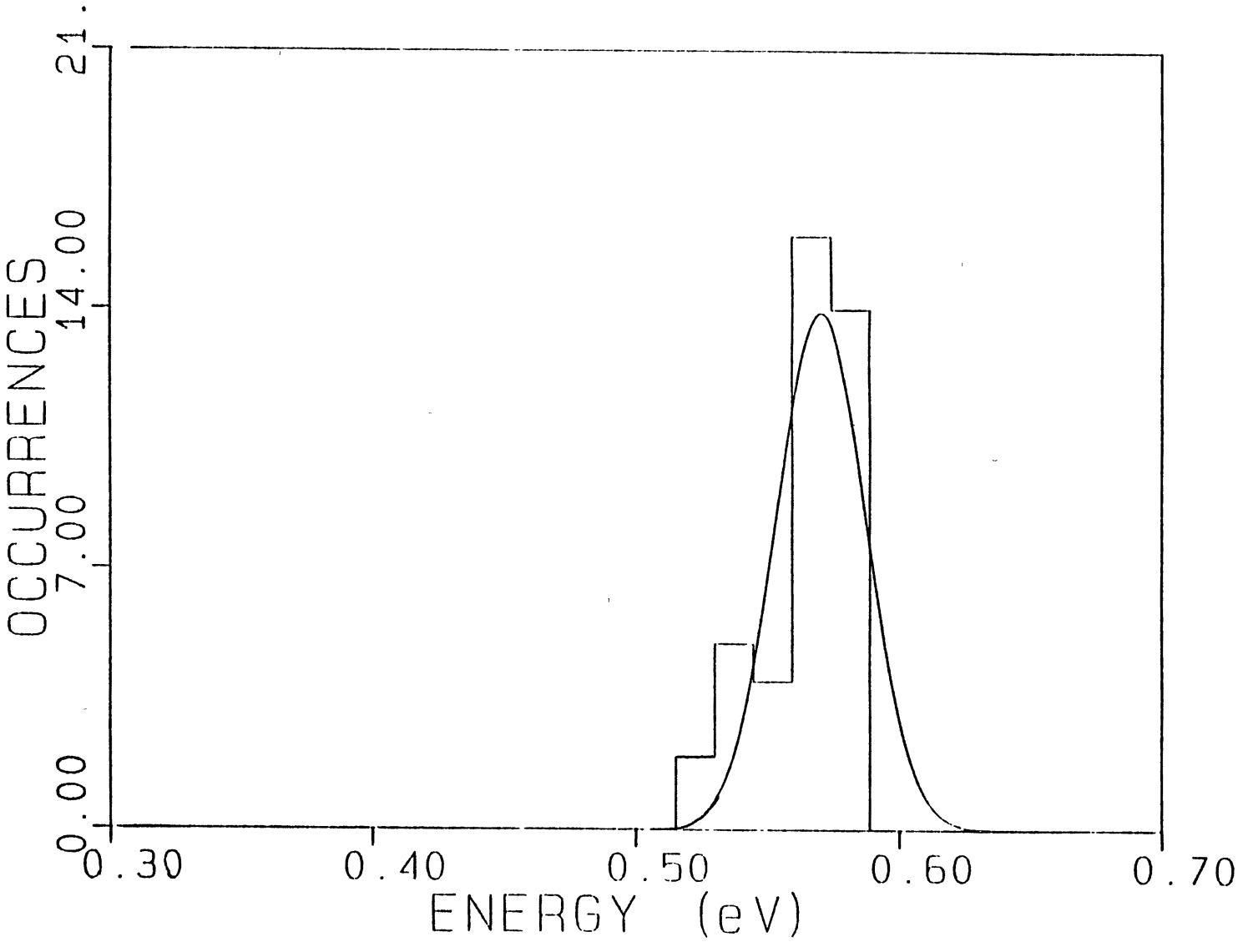

Figure 20. Plot of Number of Occurrences vs. Recoil Energy for Ar at 0.660 eV.

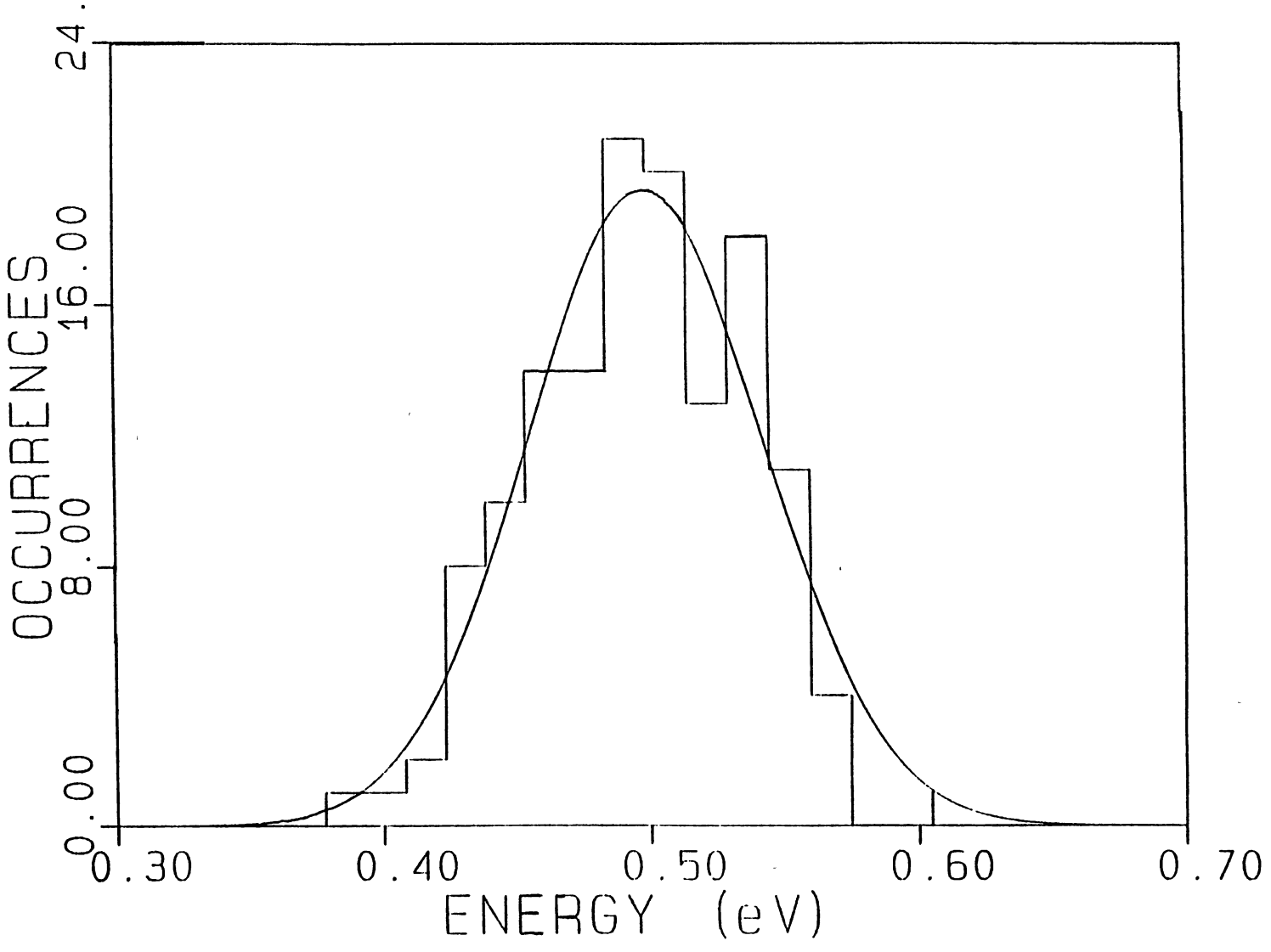

Figure 21. Plot of Number of Occurrences vs. Recoil Energy for Kr at 0.609 eV.

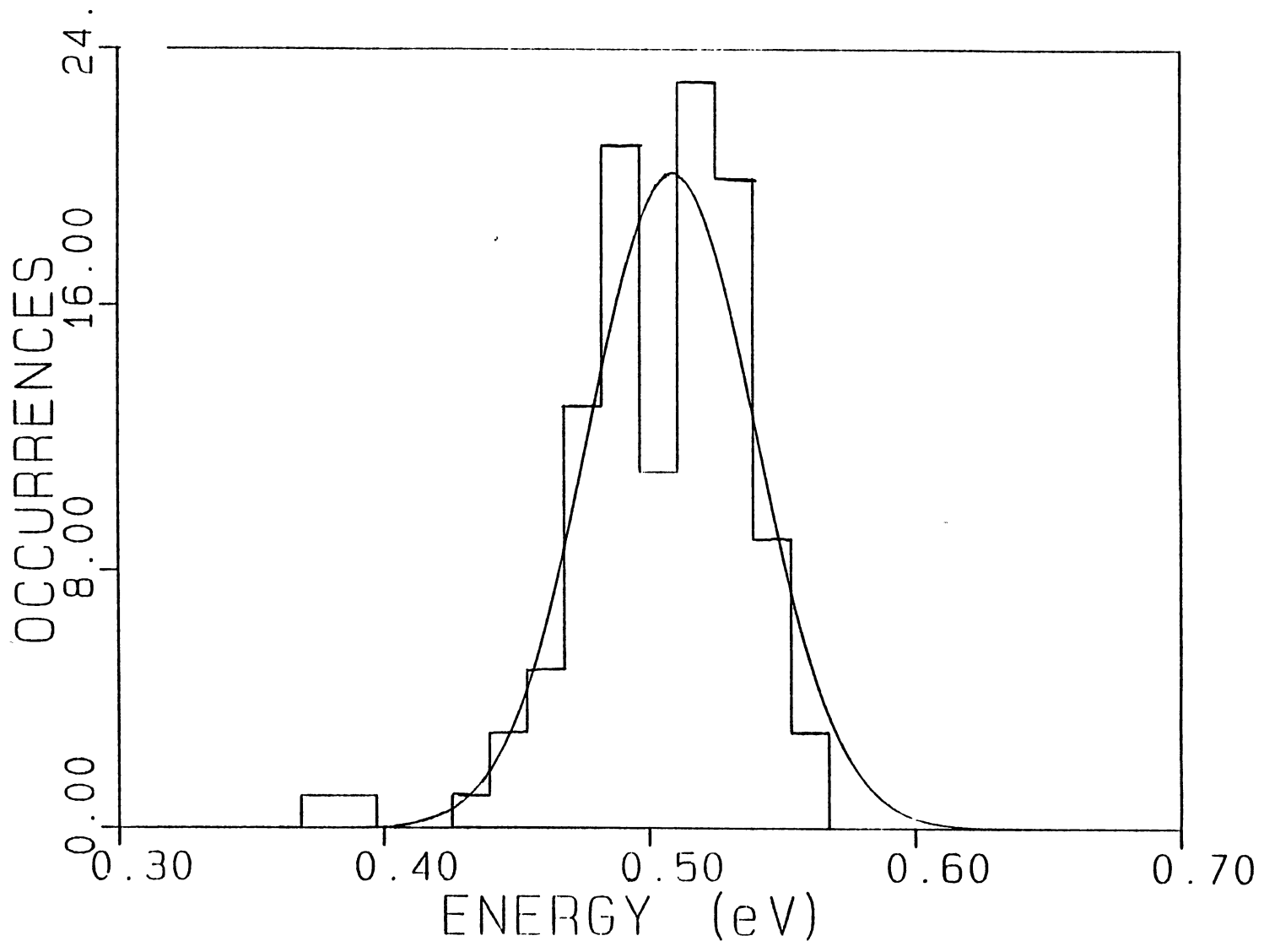

Figure 22. Plot of Number of Occurrences vs. Recoil Energy for Kr at 0.620 eV.

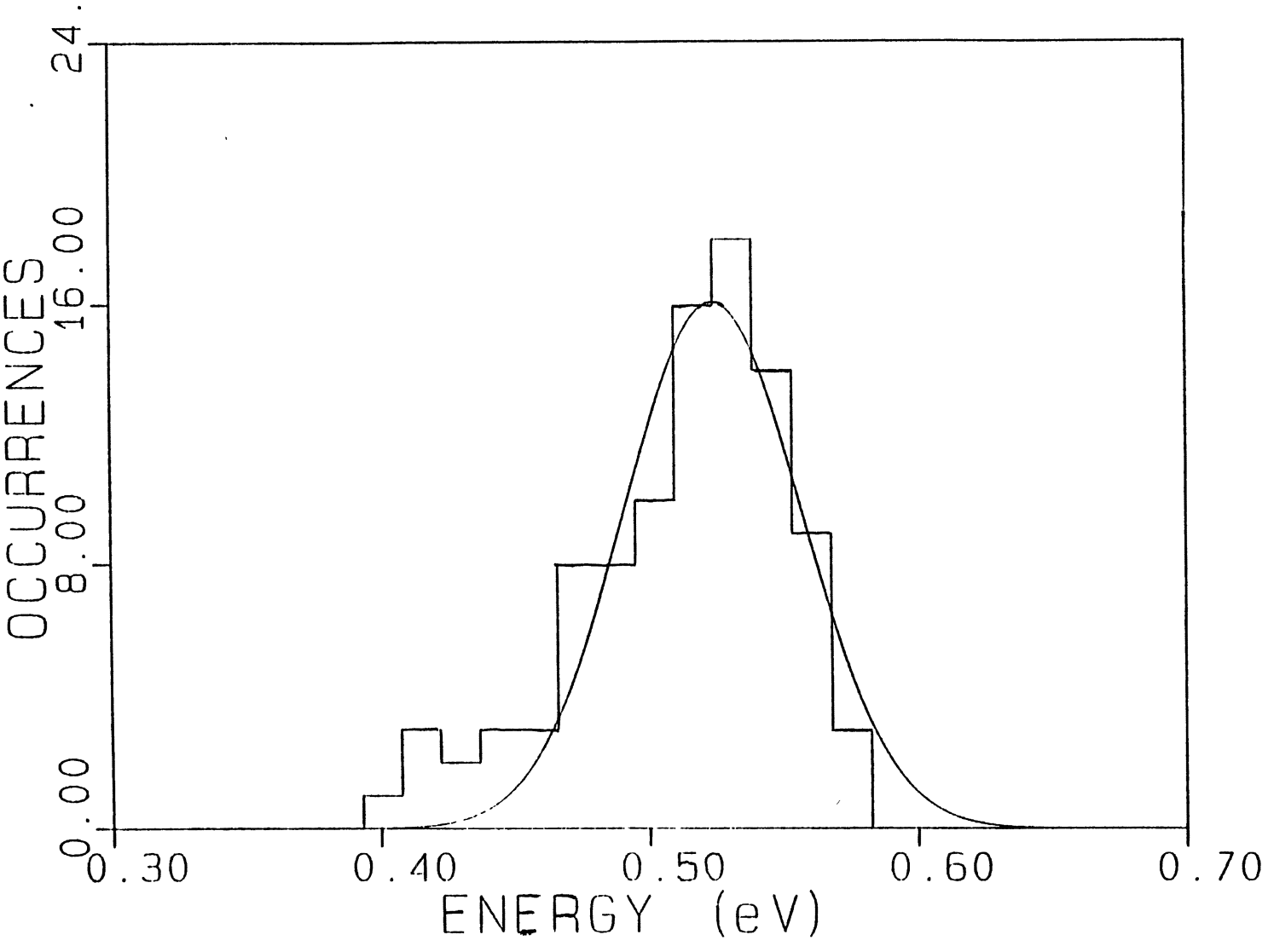

Figure 23. Plot of Number of Occurrences vs. Recoil Energy for Kr at 0.640 eV.

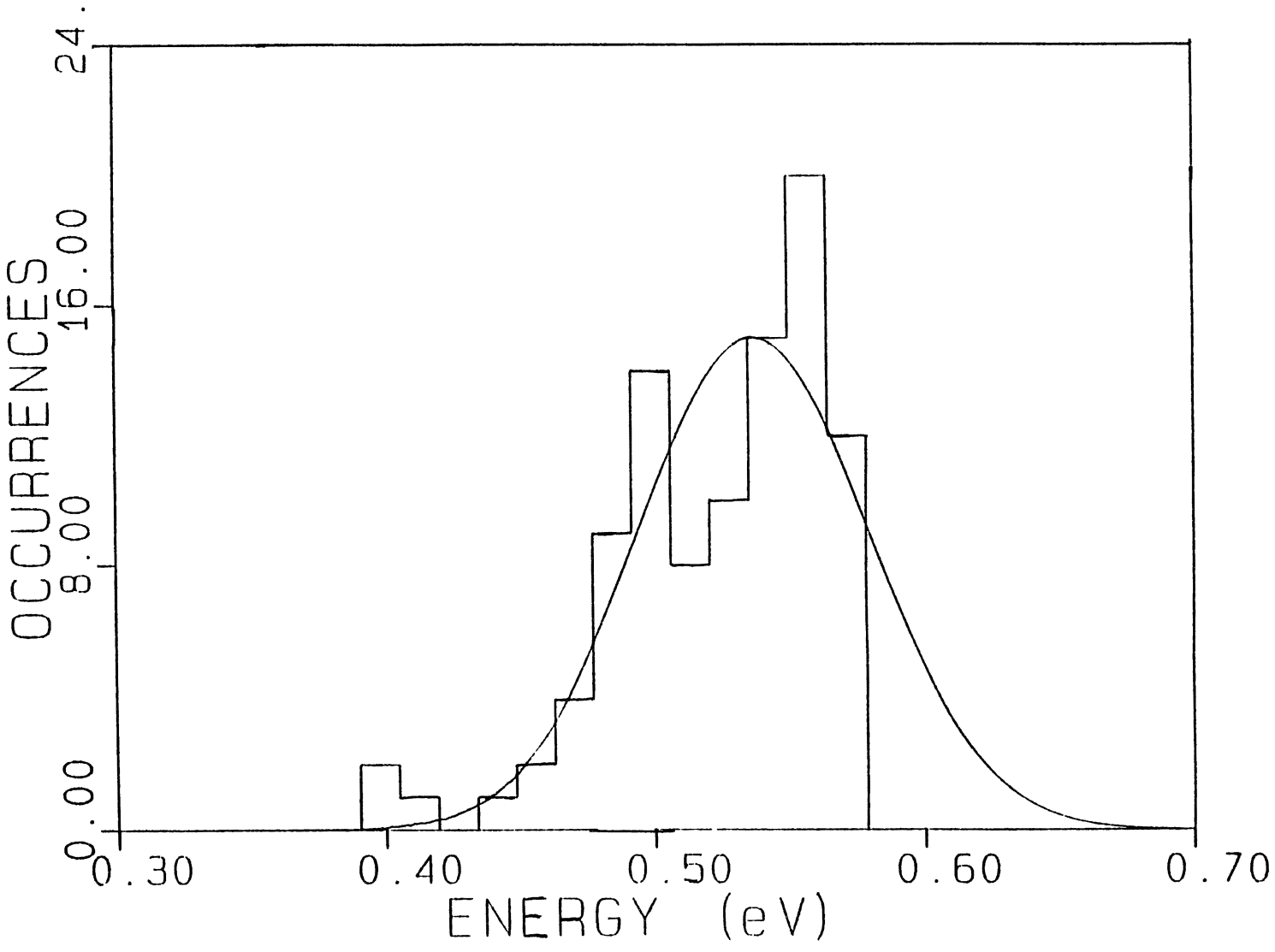

Figure 24. Plot of Number of Occurrences vs. Recoil Energy for Kr at 0.660eV.

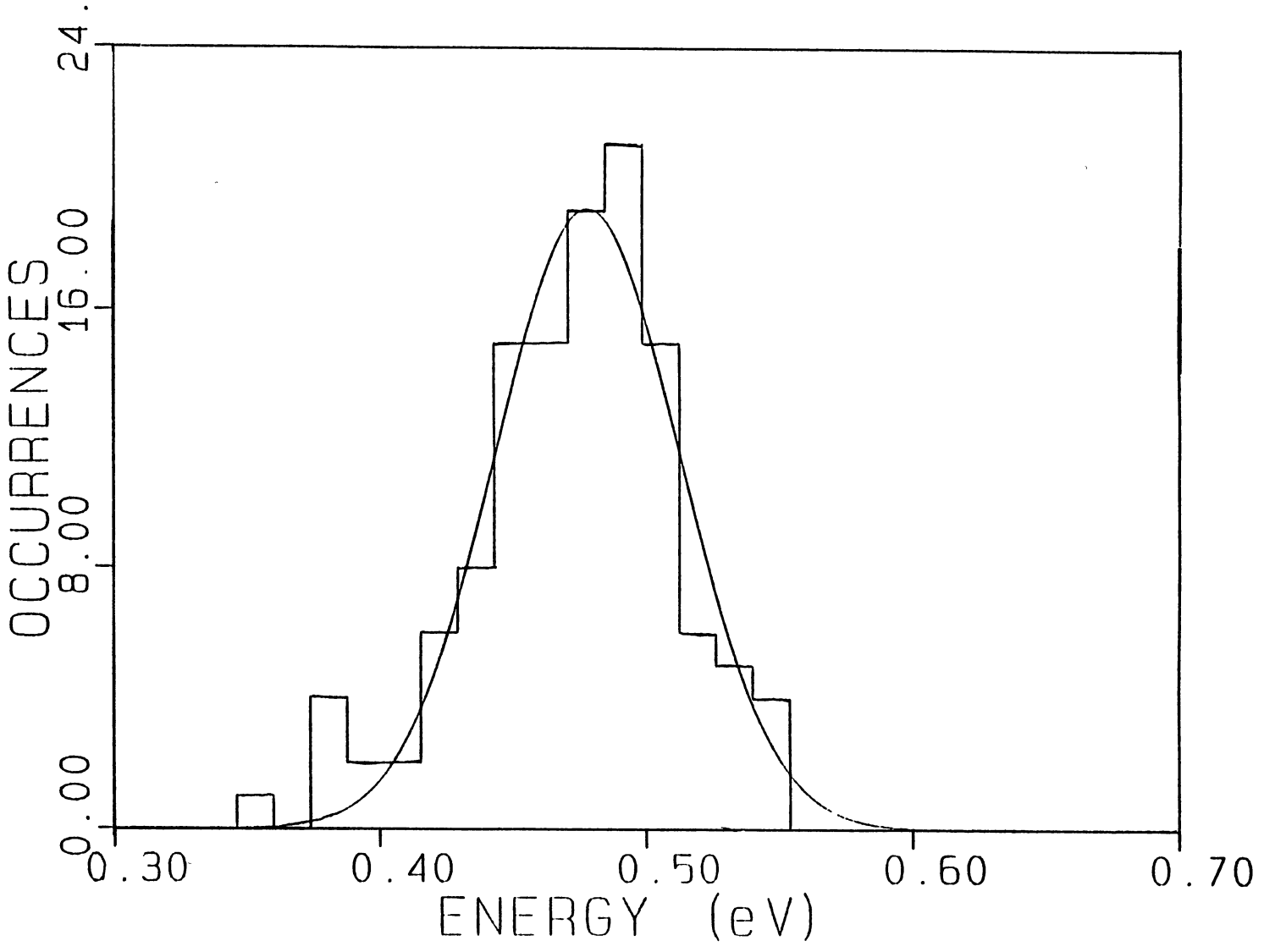

Figure 25. Plot of Number of Occurrences vs. Recoil Energy for Xe at 0.609 eV.

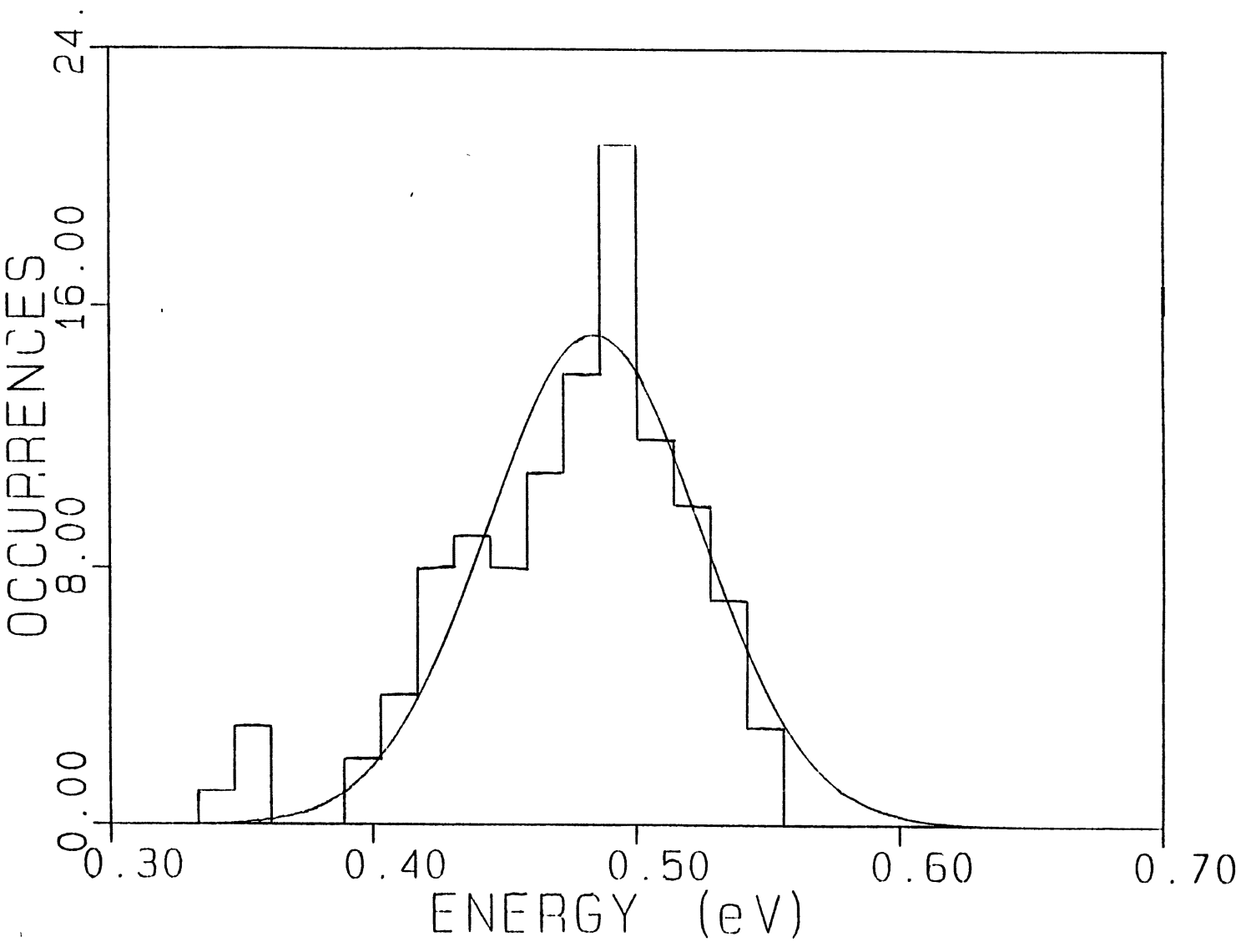

Figure 26. Plot of Number of Occurrences vs. Recoil Energy for Xe at 0.620 eV.

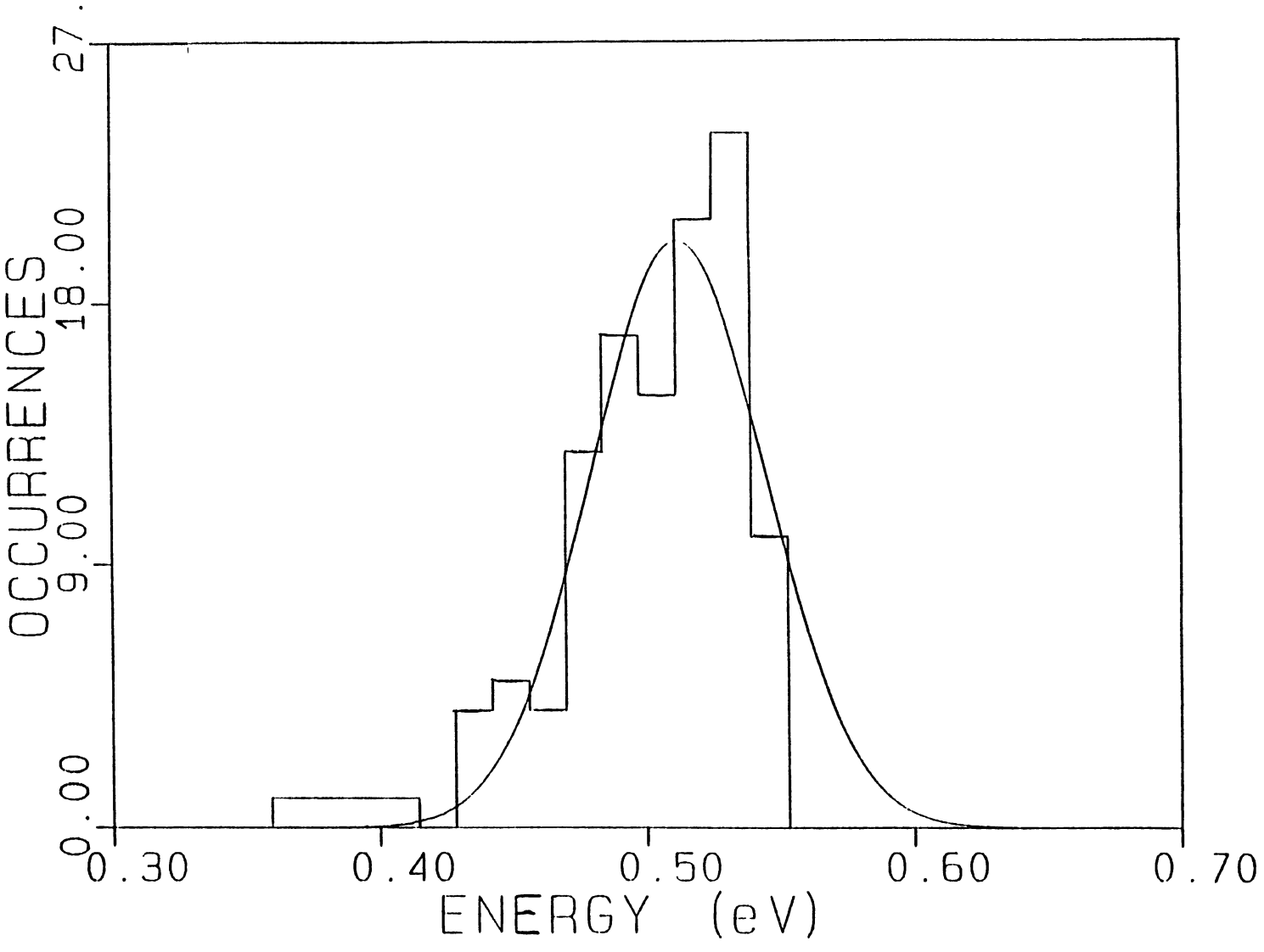

Figure 27. Plot of Number of Occurrences vs. Recoil Energy for Xe at 0.640 eV.

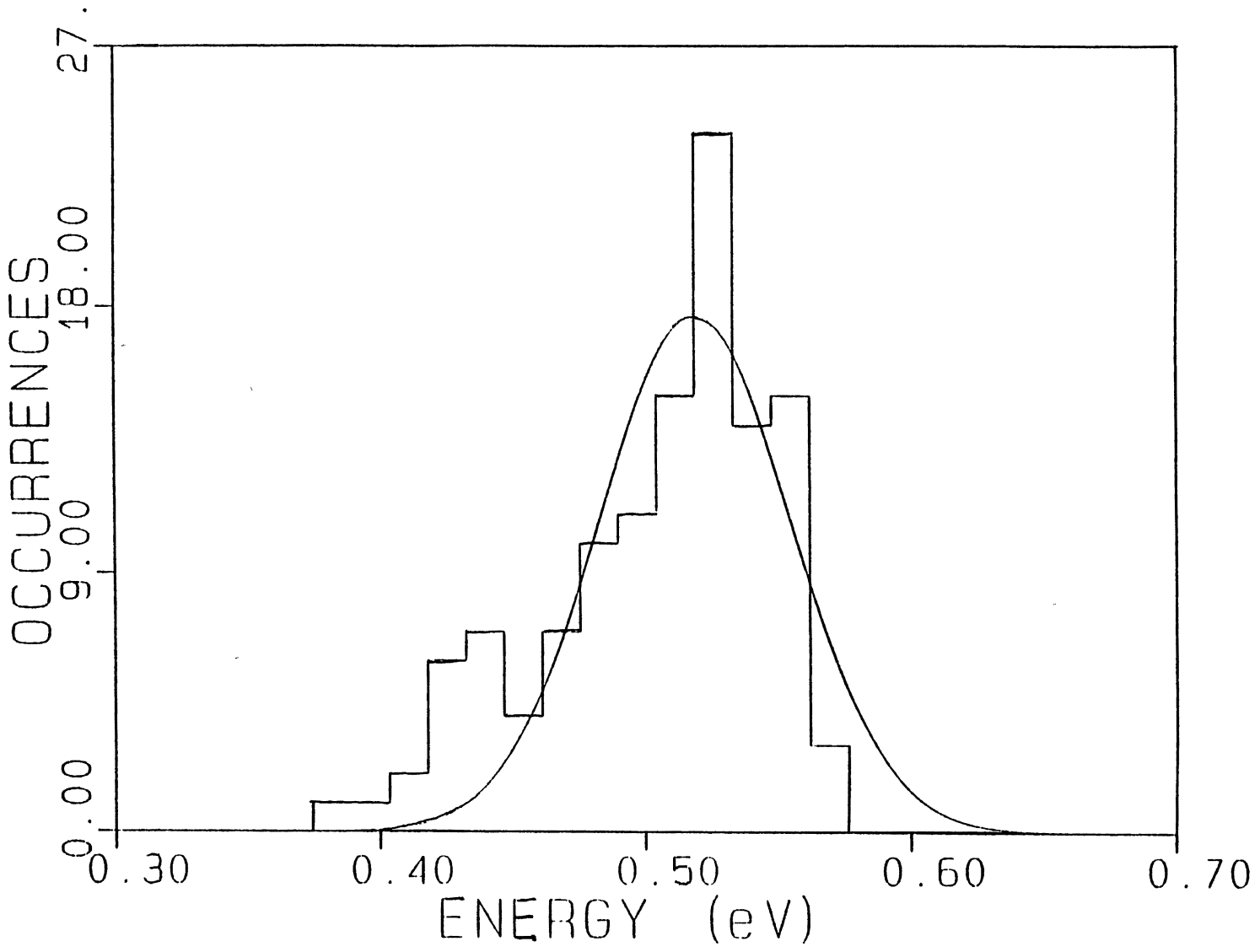

Figure 28. Plot of Number of Occurrences vs. Recoil Energy for Xe at 0.660 eV.

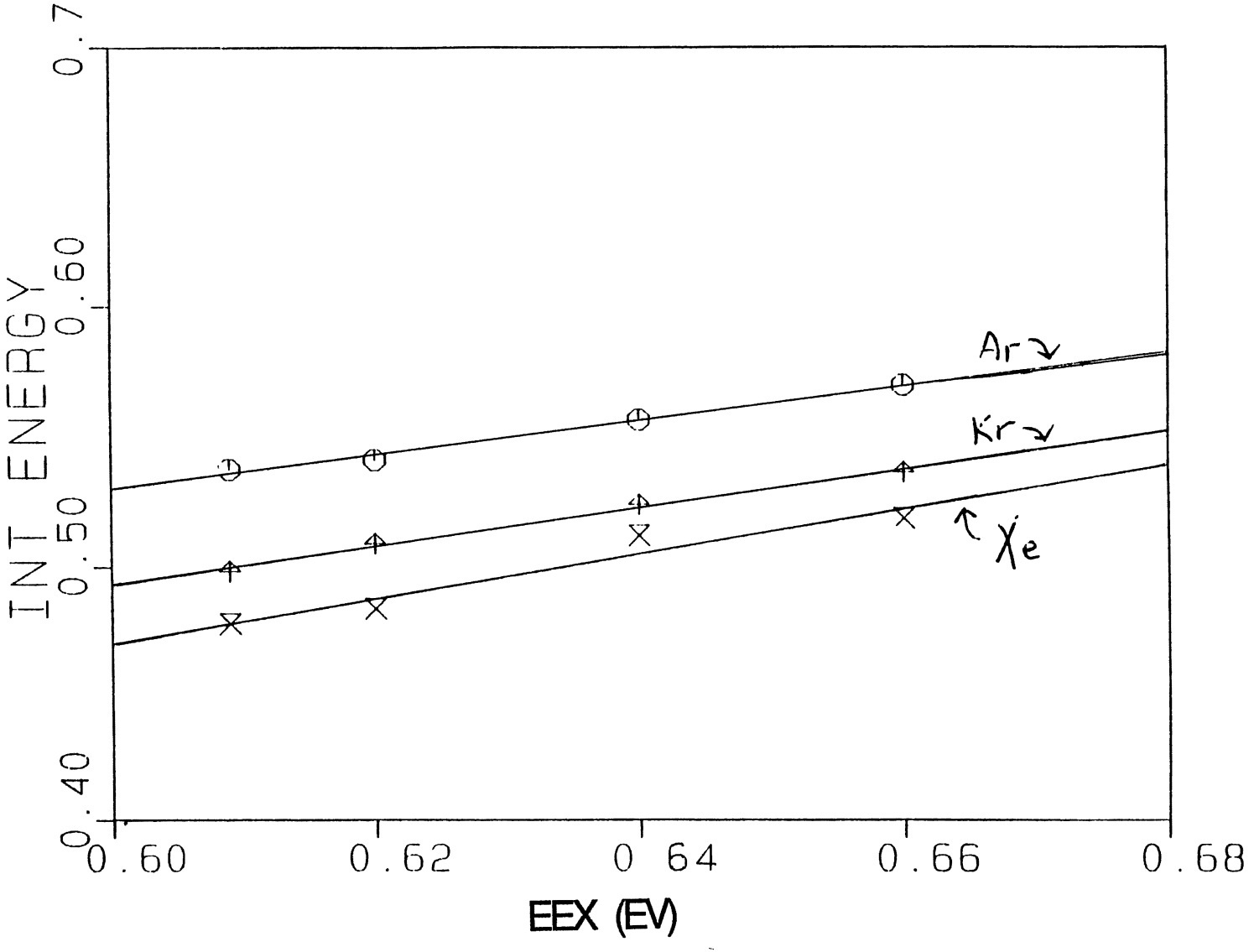

Figure 29. Plot of Internal Energy vs. Excitation Energy for Ar, Kr, and Xe.

BIBLIOGRAPHY

(1) P. Hobza and R. Zahradnik, "Weak Intermolecular Interactions in Chemistry and Biology",(Elsevier, New York, 1980)

(2) D.H. Levy, Adv. Chem. Phys., 47, 33 (1984)

(3) J.A. Blazy, B.M. DeKoven, T.D. Russell, and D.H. Levy, J. Chem. Phys. 72, 2439 (1980)

(4) K.E. Johnson, L. Wharton, and D.H. Levy, J. Chem. Phys. 69, 2719 (1978)

(5) R.E. Smalley, D.H. Levy, and L.Wharton, J. Chem. Phys. 64, 3266 (1976)

(6) W. Sharfin, K.E. Johnson, L. Wharton, and D.H. Levy, J. Chem. Phys. 71, 1292 (1979)

(7) K.E. Johnson, W. Sharfin, and D.H. Levy, J. Chem. Phys. 74, 163 (1981)

(8) J.A. Beswick and J. Jortner, J. Chem. Phys. 68, 2277 (1978)

(9) (a) P. Villarreal, G. Delgado-Barrio, and P. Mareca, J. of Mol. Struct., 120, 303 (1985)

(b) N. Martin, P. Villarreal, and G. Delgado-Barrio, J. of Mol. Struct., 120, 297 (1985)

(10) N. Halberstadt, J.A. Beswick, and K.C. Janda, J. Chem. Phys., 87, 3966 (1987)

(11) S.B. Woodruff and D.L. Thompson, J. Chem. Phys. 71, 376 (1979)

(12) J. Frank and E. Rabinowitch, Trans. Faraday Soc., 30, 120 (1934)

(13) J.N. Murrell, A.J. Stace, and R. Damnel, J. Chem. Soc. Faraday Trans. 2 78, 1532 (1978)

(14) K.L. Saenger, G.M. McClelland, and D.R. Herschbach, J. Phys. Chem., 85, 3333 (1981)

(15) J.J. Valentini and J.B. Cross, J. Chem. Phys., 77, 572 (1982)

(16) I. Noorbatcha, L.M. Raff, and D.L. Thompson, J. Chem. Phys. 81, 5658 (1984)

(17) G. Schatz, V. Buch, M.A. Ratner, R.B. Gerber, J. Chem. Phys., 79, 1808 (1983)

(18) J.M.Philippoz, J. van den Bergh, and R. Monot, J. Chem. Phys., 91, 2545 (1987)

(19) L.M. Raff and D.L. Thompson, in "Theory of Chemical Reaction Dynamics", edited by M. Baer (Chemical Rubber, Boca Raton, Fl. 1984)

(20) Robert E. Howard, Robert E. Roberts, and Michael J. DelleDonne J. Chem. Phys., 65, 3067, (1976)

(21) Ludwig W. Bruch and Ian J. McGee, J. Chem. Phys. 46, 2959, (1967)

(22) Donald L. Thompson and L.M. Raff, J. Chem. Phys., 76, 301, (1982)

(23) Randy A. Turner, L.M. Raff, and Donald L. Thompson, J. Chem. Phys., 80, 3189, (1984)

VITA

Jeffrey C. Fuson

Candidate for the Degree of

Master of Science

Thesis: THE UNIMOLECULAR DISSOCIATION OF Rg_2I_2 Rg = (He, Ar, Kr, Xe)

Major Field: Chemistry

Biographical:

Personal Data: Born in Lubbock, Texas, August 18, 1955, the son of Frank C. and Naoma Fuson.

Education: Graduated from Norman High School, Norman, Oklahoma, in May 1973; received Bachelor of Science Degree in Chemistry from University of Oklahoma in May 1981; completed requirements for the Master of Science degree at Oklahoma State University in December, 1991.

Professional Experience: Teaching Assistant, Department of Chemistry, Oklahoma State University, August, 1986, to December, 1990.